In-Situ and Experimental Evidence for Acidic Weathering of Rocks and Soils on Mars

Hurowitz, J.A.[1*], McLennan, S.M.[1], Tosca, N.J.[1], Arvidson, R.E.[2], Michalski, J.R.[3], Ming, D.W.[4], Schröder, C.[5], Squyres, S.W.[6]

[1]Department of Geosciences, State University of New York at Stony Brook, Stony Brook, NY 11794-2100

[2]Department of Earth and Planetary Sciences, Washington University, St. Louis, MO

[3]Department of Geological Sciences, Arizona State University, Tempe, AZ

[4]NASA Johnson Space Center, Houston, TX

[5]Institut für Anorganische und Analytische Chemie, Johannes Gutenberg-Universität, Staudinger Weg 9, D-55128 Mainz, Germany

[6]Department of Astronomy, Cornell University, Ithaca, NY

*Author to whom correspondence should be addressed: joel.hurowitz@stonybrook.edu

Phone: (631) 632-1936

Fax: (631) 632-8240

Abstract: Experimental data for alteration of synthetic Martian basalts at pH=0-1 indicate that chemical fractionations at low pH are vastly different from those observed during terrestrial weathering. Rock analyses from Gusev crater are well described by the relationships apparent from low pH experimental alteration data. A model for rock surface alteration is developed which indicates that a leached alteration zone is present on rock surfaces at Gusev. This zone is not chemically fractionated to a large degree from the underlying rock interior, indicating that the rock surface alteration process has occurred at low fluid-to-rock ratio. The geochemistry of natural rock surfaces analyzed by APXS is consistent with a mixture between adhering soil/dust and the leached alteration zone. The chemistry of rock surfaces analyzed after brushing with the RAT is largely representative of the leached alteration zone. The chemistry of rock surfaces analyzed after grinding with the RAT is largely representative of the interior of the rock, relatively unaffected by the alteration process occurring at the rock surface. Elemental measurements from the Spirit, Opportunity, Pathfinder and Viking 1 landing sites indicate that soil chemistry from widely separated locations is consistent with the low-pH, low fluid to rock ratio alteration relationships developed for Gusev rocks. Soils are affected principally by mobility of FeO and MgO, consistent with alteration of olivine-bearing basalt and subsequent precipitation of FeO and MgO bearing secondary minerals as the primary control on soil geochemistry.

Introduction: The petrography, mineralogy and geochemistry of sedimentary rocks have long been utilized for the reconstruction of environmental conditions in the Earth's past [e.g., *McLennan et al.*, 1993; *Nesbitt and Young*, 1982; *Patchett et al.*, 1999]. The chemical and mineralogical changes that accompany weathering of the Earth's crust have been studied in great detail in order to better understand the processes controlling the composition of sedimentary rocks [*Nesbitt and Markovics*, 1997; *Nesbitt and Young*, 1984; *Nesbitt et al.*, 1996]. In particular, the weathering of granodiorite has received much attention, since the Earth's upper continental crust is known to be, on average, of granodioritic composition [*McLennan*, 2001; *Taylor and McLennan*, 1985]. Although it has received less consideration, the weathering of basaltic rocks on Earth has been studied as well, and there is a reasonable understanding of the bulk chemical and mineralogical changes that accompany the alteration of such rocks under terrestrial conditions [*Eggleton et al.*, 1987; *Gislason and Eugster*, 1987; *Gislason et al.*, 1996; *Nesbitt and Wilson*, 1992]. With the advent of *in situ* geochemical and mineralogical study of Martian rocks, it has recently become possible to investigate the alteration of rocks, primarily basalts, on that planet. Interestingly, altered Martian rocks and soils do not appear to have evolved in a manner consistent with alteration of basalts as we know it on Earth [*McSween et al.*, 2003; *McSween and Keil*, 2000].

Here we present new findings regarding weathering processes on Mars utilizing the results of alteration experiments performed at low-pH on synthetic basalts of Martian composition [*Hurowitz et al.*, in press; *Tosca et al.*, 2004]. These experimental results indicate that weathering in the low pH environment now thought to be likely for Martian surface waters [*Haskin et al.*, in press; *Squyres et al.*, 2004; *Tosca et al.*, in press] results

in alteration products that do not evolve in a similar manner to weathering profiles on Earth. Instead, the primary processes thought to control the composition of altered materials on Mars, namely acid alteration and secondary sulfate and Fe-oxide formation, produce weathering products whose chemical composition does not lend itself to comparison with terrestrial weathering products.

In this paper, we present a brief overview of the primary controls on the major element chemistry of weathering profiles generated on Earth, followed by a comparison to the results of low-pH alteration experiments. These experimental results are then applied to understanding rock surface alteration profiles exposed using the Rock Abrasion Tool (RAT) [*Gorevan et al.*, 2003], and analyzed using the Alpha Particle X-ray Spectrometer (APXS) [*Rieder et al.*, 2003], onboard the Spirit rover at Gusev crater. Finally, soil chemistry from the Spirit, Opportunity, and Sojourner rovers, as well as the Viking 1 lander, are examined in light of the insights gained by examination of rock weathering at Gusev.

Discussion I – The Effect of pH on Weathering Relationships

Terrestrial Weathering: Figure 1 is a ternary diagram that plots the mole fractions of FeO_T + MgO, Al_2O_3, and CaO + Na_2O + K_2O at the apices. The compositions of many important primary igneous and secondary alteration minerals are plotted on Figure 1, with most of the phases having distinct locations on the diagram. This separation among phases makes this diagram particularly useful for visualizing mixing and mass balance relationships, as well as for tracking alteration pathways during weathering. These types of diagrams have been successfully utilized to predict the major element and

mineralogical composition of weathering profiles generated on primary igneous rocks at the Earth's surface [*Fedo et al.*, 1995; *Nesbitt and Young*, 1982; *Nesbitt et al.*, 1996], and will be utilized throughout this paper.

Plotted on Figure 1 are data for weathering profiles generated on the Baynton basalt [*Nesbitt and Wilson*, 1992] and the Toorongo granodiorite [*Nesbitt and Markovics*, 1997]. Both weathering profiles are developed in temperate climates in Australia (700-1500 mm average annual rainfall, seasonal temperature range -5^{o}C to 38^{o}C), and demonstrate the chemical and mineralogical changes that can take place as basalt and granodiorite are weathered at the Earth's surface. Also plotted on Figure 1 are a number of Martian rock compositions.

As shown on Figure 1, the primary compositional variability of the various basaltic igneous rocks follows a trend subparallel to a tie line drawn between feldspar and the FeO_T + MgO apex. This is a result of the fact that, for the elements plotted, the basalts represent mixtures of feldspar, olivine, pyroxene, and Fe-Ti oxides. The Toorongo granodiorite represents a mixture of feldspar, biotite, amphibole, and Fe-Ti oxides. The weathering trends (shown by the arrows on Figure 1), indicate that the main consequence of weathering at the Earth's surface is to leach primary igneous minerals of the soluble elements Ca, Na, Mg, and to a lesser extent K, while enriching the weathering profile in the insoluble elements Al and Fe (in the form of Fe (III)). As a consequence of the leaching process, natural waters become enriched in soluble elements and evolve towards the lower left hand apex of Figure 1. As discussed below, these weathering trends develop primarily as a result of one major factor: the pH of the waters which are altering primary igneous rocks at the Earth's surface.

With the exception of rare acidic regimes (hydrothermal systems, acid-saline lakes), subaerial alteration on Earth primarily occurs as rainwater percolates through the subsurface. The pH of "pristine" rainwater is buffered by carbonic acid equilibria at pH 5.65, and is typically elevated in groundwater to near neutral pH by acid buffering reactions with minerals. In areas of high rainfall where the acid neutralizing capability of the local soil and bedrock has been exceeded (e.g., Hawaiian rainforest soils) groundwater typically has a pH of 5-6 [*Patterson*, 1971]. In areas where little acidity is available and chemical alteration of basaltic glass has taken place (e.g., sparsely vegetated regions in Iceland), groundwater can attain pH values as high as 9-10, at which point saturation with respect to some igneous minerals is attained [*Gislason and Arnorsson*, 1993].

In Figures 2A and 2B the speciation of Al and Fe (III) in solution is plotted on diagrams of log activity versus pH. The pH values of most natural terrestrial waters (~5-9) fall at or near the solubility minima of Al and Fe (III) with respect to the secondary mineral phases kaolinite and goethite, respectively. These are two common secondary minerals in terrestrial weathering profiles developed on basaltic bedrock [*Gislason et al.*, 1996; *Karrat et al.*, 1998; *Nesbitt and Wilson*, 1992]. The relationships shown on Figures 2A and 2B indicate that as primary mineral dissolution occurs under normal terrestrial conditions, little Al or Fe (III) can be accommodated in solution (compared to low pH fluids) before saturation with respect to secondary phases is reached. Once saturation with respect to secondary phases is attained, precipitation of those phases is thermodynamically favorable.

Another important factor controlled by pH is the rate at which Fe (II) released to solution oxidizes to Fe (III). The rate of iron oxidation increases 100-fold for every unit increase in pH at pH values greater than about 4, whereas the rate of iron oxidation is constant for pH less than about 4, as shown on Figure 2C. As a result of this rate dependence on pH, any Fe (II) released to solution oxidizes rapidly to insoluble Fe (III) under the pH conditions of most natural waters on Earth.

As demonstrated by Figures 2A-C, Al and Fe (III) solubility are low and the rate of Fe (II) oxidation is rapid in terrestrial groundwaters. The end result of these pH-driven effects is that as alteration occurs, any Al and Fe released to solution from primary mineral dissolution rapidly precipitates out in the form of aluminum- and ferric iron-bearing secondary minerals. The soluble elements Mg, Ca, Na, and K are leached from the weathering profile due to their relatively high solubility. This combination of leaching and precipitation results in a passive enrichment in both total Fe and Al, as indicated by the weathering trends on Fig. 1. If weathering on Mars were to have taken place under pH conditions similar to those on Earth, we might expect the altered rocks and soils analyzed on Mars to evolve in a geochemically similar manner, with the altered materials being enriched in total Fe and Al relative to the unaltered igneous rocks from which they are derived.

Experimental Weathering at Low pH: It is generally accepted that the high concentrations of S and Cl in Martian soils are consistent with the presence of a salt component formed in a low-pH environment rich in acidic sulfate and chloride species [*Burns*, 1987; *Clark and Van Hart*, 1981; *Newsom et al.*, 1999]. This salt component appears to be a

ubiquitous feature of soils and rocks analyzed at widely separated geographical locations on the Martian surface [*Clark et al.*, 1982; *Foley et al.*, 2003; *Gellert et al.*, 2004; *Rieder et al.*, 2004]. This had led some early workers to propose that aqueous fluids are dominantly acidic in the Martian surface and shallow subsurface [*Banin et al.*, 1997; *Burns*, 1993; *Burns and Fisher*, 1993; *Settle*, 1979], a hypothesis which has been confirmed by geochemical analyses at both the Opportunity [*Klingelhöfer et al.*, 2004; *Squyres et al.*, 2004; *Tosca et al.*, in press] and Spirit [*Haskin et al.*, in press; *Ming*, 2005; *Morris et al.*, 2005] landing sites. In experimental studies by Hurowitz et al. [in press] and Tosca et al. [2004], synthetic basalts of Martian composition were experimentally altered under low-pH conditions (pH ~0-3.5) in order to ascertain the nature of the secondary minerals produced by alteration of Martian basalts in acidic environments.

From these studies, the composition of the basaltic residue remaining from alteration at low pH can be calculated from the composition of the starting basalt (as determined by ion microprobe) and the fluid compositions produced during alteration (as determined by argon emission spectroscopy). These calculated residual compositions can then be utilized to ascertain the nature of chemical fractionation during low-pH alteration processes for the purpose of comparison to Martian rocks and soils. The results of these calculations are shown on Table 1 and Figures 3 and 4. We emphasize the results of the lowest pH and highest fluid-to-rock ratio experiments from these two studies because they generate the largest differences in chemical composition between primary basalt and altered residue.

From the results of Hurowitz et al. [in press], data for the alteration of an olivine-free synthetic Los Angeles basaltic shergottite at pH = 1.0 and fluid to rock ratio = 1000

is shown on Figure 3. As discussed in their study, dissolution of the primary mineral phases labradorite and titanomagnetite dominates the solution chemistry, and as a result, the calculated residual basalt becomes depleted in Al, Na, Ti, and Ca. Due to its slow dissolution rate relative to labradorite and titanomagnetite under these conditions, clinopyroxene remained relatively unaltered in the experiments. Not surprisingly then, the calculated composition of the altered residue evolves towards a composition resembling that of pyroxene (Fig. 3). The calculated mass loss from the original basalt is ~50% (Table 1).

From the results of Tosca et al. [*Tosca et al.*, 2004], data for the alteration (pH = 0, fluid to rock ratio = 10) of an olivine-bearing synthetic basalt having a composition based on S-and Cl-free Pathfinder soil analyses is shown on Figure 4 (see Tosca et al. [2004] for a discussion of this composition). As discussed in that study, the dissolution of the primary mineral phase olivine dominates the solution chemistry, and as a result, the calculated residual basalt becomes depleted in Mg and Fe. The calculated mass loss from the original basalt is ~20% (Table 1).

For less acidic initial pH conditions than those utilized in our calculations, one should expect to see qualitatively similar changes in bulk rock chemical composition to those shown on Figures 3 and 4. For pH conditions anywhere between about 0-4 there should be no change in the behavior of Fe^{2+} leached from basalt since the rate of Fe-oxidation is pH independent in this range (Fig. 2C). That is, Fe oxidation kinetics are invariant from pH 0-4, and so the passive Fe enrichment common to terrestrial weathering profiles (Fig. 1), which results from the rapid oxidation and precipitation of insoluble Fe^{3+}, should not be observed. In addition, the solubility of Al^{3+} and Fe^{3+} are

substantially higher in this pH range than that seen for the circum-neutral pH typical of terrestrial alteration (Fig.s 2A and 2B). Therefore one can predict, for example, that as the initial pH of the fluid in contact with the rock being altered increases from 0 to 4, the alteration trends shown on Figures 3 and 4 should not change substantially. However, as initial pH increases, more fluid will be required to generate the same changes in rock chemistry since mineral dissolution rates decrease as pH increases from 0 to 4 [*White and Brantley*, 1995]. The details of exactly how the alteration trends shown in Figures 3 and 4 evolve from the acidic pH regime (pH ~0-4) in which Fe-oxidation kinetics are pH-independent, to the mildly acidic/neutral pH regime (pH ~4-7), is an area which requires further systematic experimental investigation.

It is clear from inspection of Figures 3 and 4 that alteration at low pH results in vastly different weathering trends than those observed for alteration under typical terrestrial conditions (compare to terrestrial weathering trends shown on Fig.s 1, 3 and 4). Al and Fe (III) are far more soluble at these low pH values than they are at the pH of groundwaters on Earth (Figs. 2A and 2B), and the rate of Fe (II) oxidation to less soluble Fe (III) is lower (Fig. 2C). Note that there is a difference in Al and Fe (III) solubility of 5 and 2 orders of magnitude, respectively, between pH 6 and 3.5 (Figs. 2A and 2B). Also, the Fe-oxidation rate decreases by 3.5 orders of magnitude between pH 6 and 3.5 (Fig. 2C). At low pH aluminum and iron are not immobile elements and chemical fractionation is dominated by mineral dissolution. As a result, basaltic residues become depleted in the elements contained in the primary minerals undergoing the most rapid alteration, which is simply a function of their relative dissolution rates.

Plotted on Figure 5 are the experimentally determined dissolution rates (pH = 2, 25^{o}C) of some primary igneous mineral phases. For the olivine-free Los Angeles basalt, the two primary phases with the fastest dissolution rate are titanomagnetite and labradorite, and both solution composition and residual basalt compositions are controlled by the dissolution of these phases (Fig. 3). The same effect is seen for the olivine bearing basalt composition of Tosca et al. [2004], in which the fastest dissolving phase is olivine (Fig. 4). This is not to say that only labradorite and titanomagnetite are dissolving from the Los Angeles basalt, and that only olivine is dissolving from the olivine-bearing basalt composition, as all of the phases in the basalt are undergoing dissolution. The acid dissolution process is not selective for one mineral versus another, but the fluid chemistry is dominated by input from the phase, or phases, that alter the most rapidly. This is an important point for later discussion of rock alteration trends at Gusev, whose geochemistry is also dominated by the dissolution of the most readily altered phases.

An interesting effect of low-pH alteration is that the trends shown for the dissolution of olivine-free and olivine-bearing basalts (Figs. 3 and 4) are subparallel to the primary compositional variability of unaltered igneous rocks (Fig. 1). This may make the effects of weathering in a low-pH environment difficult to distinguish from simple compositional heterogeneity among unaltered rocks and soils. However, as will be discussed below, the differences between rock surface and rock interior chemistry (as revealed by the RAT) can be understood in terms of the low-pH dissolution relationships just discussed.

Discussion II – Application to Martian Rocks and Soils

Rock Analyses: APXS analyses of rocks will be discussed in terms of "Surface", "Brushed", and "RATted" analyses. These represent analyses of pristine rock surfaces ("Surface"), rock surfaces which have had adhering soil and dust removed by the RAT brush ("Brushed"), and rocks which have been ground to variable depth by the RAT ("RATted"). Microscopic Imager (MI) mosaics representative of each of these types of surfaces on the rock "Humphrey" can be found in Figure 11 of Arvidson, et al., [2005], and Figure 4 of Herkenhoff et al. [2004] for the rock "Adirondack". As discussed in Gorevan et al. [2005], in order to remove adhering fines from rock surfaces the RAT uses its Rotate Brush to sweep a 45-mm diameter spot of zero depth at the rock surface. The RAT then uses its grinding wheel to grind a 45-mm diameter hole with a nominal depth of 5-mm into the rock. The actual depth of RAT grinds into rocks analyzed at Gusev ranged from approximately 2 to 9 mm, and RAT grind depths are tabulated on a rock-by-rock basis in Arvidson et al. [2005]. A summary of rock analysis operations organized by sol number can also be found in Arvidson et al. [2005].

Plains Adirondack Type Basalts: As discussed in McSween et al. [2004] the RATted rocks analyzed on the Gusev Plains (Adirondack, Humphrey, Mazatzal) are olivine-normative picritic basalts. These rocks are collectively known as "Plains Adirondack" type basalts. The rocks Adirondack and Humphrey are discussed below. The rock Mazatzal is not discussed in this report due to the presence of a thick and complex coating [*Haskin et al.*, in press; *Morris et al.*, 2004; *Schröder*, 2005] which obscures the low-pH dissolution relationships evident for Adirondack and Humphrey.

Data for the brushed and RATted surfaces of Adirondack and Humphrey are shown in Figure 6. In this, and all subsequent ternary plots discussed in this paper, the symbols occupy a space on the diagrams representing approximately ± 1.0% in "ternary space". Analytical uncertainties for the individual elements plotted are highly variable (from 0.5-72% relative). However, when recalculated and plotted on ternary diagrams, the cumulative uncertainties rarely constitute more than ± 1.0% (i.e. the error bars lie within the space occupied by the symbols). For analyses which have uncertainty > 1.0%, error bars have been plotted, for all others, no error bars are shown.

As shown in Figure 6, the brushed rock surfaces of Adirondack and Humphrey are depleted in MgO and FeO_T relative to the RATted rock interiors. These relationships indicate that the difference between the RATted and brushed compositions could plausibly be interpreted as resulting from dissolution of olivine at the rock surface. Note the similarity to the experimental dissolution trend shown in Figure 4. In both of the above cases (Adirondack, Humphrey), the small offsets in ternary space between brushed and RATted surfaces indicate a low degree of alteration. The offset between these data points is significantly smaller than that shown for the experimental alteration of olivine-bearing basalt (Fig. 4), indicating that if alteration of the Plains Adirondack basalts also took place at pH = 0, then the fluid to rock ratio was likely $<<10$. For less aggressive pH conditions, higher fluid to ratios are possible, although the small offsets between RATted and brushed analyses are still likely to result from interaction with small volumes of fluid.

The Mössbauer data from the brushed and RATted surfaces of both rocks are consistent with the olivine dissolution trend apparent from the APXS data. Assuming

that the composition of the olivine does not change between brushed and RATted surfaces, the values obtained by multiplying the olivine abundance derived from Mössbauer by the FeO_T content from APXS indicates that the amount of iron associated with olivine decreases from the brushed to RATted surfaces of Adirondack and Humphrey [*Gellert et al.*, 2005; *Klingelhöfer*, 2004; *Morris et al.*, 2004; *Rieder*, 2004; *Schröder*, 2005]. It is important to note, however, that caution is warranted in combining Mössbauer and APXS data because their respective radiation sources have different penetration depths [*Klingelhöfer et al.*, 2003; *Rieder et al.*, 2003].

West Spur Clovis Type Rocks: The RATted rocks analyzed at the West Spur region of Husband Hill (Clovis, Ebenezer) are collectively known as "West Spur Clovis" type rocks. For a thorough discussion of the possible origins of these rocks, see Ming et al. [2005], Morris et al. [2005], and Squyres et al. [2005], who interpret these rocks to be more pervasively altered rocks than the Plains Adirondack basalts. From the standpoint of Mössbauer spectroscopy, these rocks are highly oxidized, characterized primarily by abundant Fe-oxides and lesser pyroxene (~12-15% of Mössbauer component area), and only trace olivine (~1% of Mössbauer component area) [*Klingelhöfer*, 2004; *Morris et al.*, 2005].

On Figure 7, the data for the brushed and RATted surfaces of Clovis and Ebenezer are shown. Similar to the Plains Adirondack type basalts, the brushed rock surfaces of Clovis and Ebenezer are depleted in MgO and FeO_T relative to the RATted rock interiors, with relatively small offsets between brushed and RATted analyses. These relationships indicate that the brushed surfaces of these rocks have undergone the same

type of surface alteration process as the Plains Adirondack basalts, resulting in the loss of an Fe-Mg rich phase. In this case, Mössbauer spectroscopy does not indicate the presence of significant olivine, so this is probably not the phase controlling the apparent loss of MgO and FeO_T from the rock surface. The Mössbauer spectrometer does indicate the presence of pyroxene in these rocks and dissolution of pyroxene results in an alteration trend similar to that of the olivine dissolution trend (see Fig. 7). Making the same assumptions about mineral composition discussed for the Plains Adirondack basalts, the amount of iron associated with pyroxene decreases slightly from the brushed to RATted surfaces of Clovis, consistent with pyroxene dissolution. No brushed rock Mössbauer analysis was made on the rock Ebenezer.

Another possibility is that the observed trends result from alteration of basaltic glass. As shown on Figure 7, alteration of glassy basaltic tephras in acidic environments in Hawaii (solfatetic tephras of Morris et al. [2000]) results in alteration trends similar to those observed for the West Spur Clovis rocks. Supporting such an interpretation, deconvolution of miniature thermal emission spectrometer (Mini-TES) spectra from rocks of the West Spur region indicates a high abundance of a short-order aluminosilicate phase [*Ruff et al.*, 2005]. This identification could be indicative of fresh basaltic glass and/or a poorly crystalline alteration phase (such as allophane) which could be derived from the weathering of basaltic glass [*Michalski et al.*, 2005a; *Michalski et al.*, 2005b; *Ruff et al.*, 2005].

Husband Hill Wishstone and Cumberland Ridge Watchtower Type Rocks: The RATted rocks Champagne and Wishstone analyzed during the traverse between the West Spur

and Cumberland Ridge regions of Husband Hill are collectively known as Husband Hill Wishstone type. The rock Cumberland Ridge Watchtower is the only one of its type to have both brushed and RATted analyses, and it will be discussed in this section as well. As discussed in Arvidson et al. [2005], Champagne and Wishstone are not in-place outcrops, but Watchtower is an outcrop. These two rock types (Husband Hill Wishstone and Cumberland Ridge Watchtower) differ in a number of important aspects including FeO_T, MgO, and SO_3 concentrations, Fe mineralogy, and Fe-oxidation state [*Gellert et al.*, 2005; *Klingelhöfer*, 2004; *Morris et al.*, 2005; *Rieder*, 2004; *Squyres et al.*, 2005]. However, both rock types are similar in that they are characterized by Cr_2O_3 concentrations which are below the APXS detection limit, high concentrations of TiO_2 (2.21-2.96 weight %) and high concentrations of P_2O_5 (4.7-5.5 weight %) with a strong positive correlation between P_2O_5 and CaO, suggesting that the P_2O_5 is present as a Ca-phosphate phase [*Ming*, 2005]. In addition, both rock types appear to be affected by a similar rock surface alteration process, and for this reason, these two rocks types are grouped together in the following discussion.

On Figure 8, the data for the brushed and RATted surfaces of Champagne, Wishstone and Watchtower are shown. The brushed surfaces of all three rocks are depleted in CaO relative to corresponding RATted surfaces. Assuming that much of the CaO in these rocks is present as a phosphatic phase, the depletion of CaO could be due to dissolution of a Ca-phosphate mineral. Different Ca-phosphate phases (e.g., apatites, merrillites) cannot be readily distinguished on Figure 8, as they all plot at or near the CaO apex of the diagram.

In order to ascertain the nature of the phosphatic phase being removed from these rock surfaces, the brushed and RATted data points have been plotted on Figure 9, a ternary diagram which plots the mole fractions of CaO, P_2O_5, and the sum of MgO, FeO_T, Na_2O, and K_2O at the apices. On Figure 9, all of the primary igneous phases plot along the bottom of the ternary, while various Ca-phosphates plot along the CaO-P_2O_5 join. As shown, the brushed surfaces are depleted in CaO and P_2O_5 relative to the RATted surfaces, and the depletion is consistent with the removal of a phosphate mineral having a higher P_2O_5: CaO ratio than apatite, possibly phases such as monetite, brushite, or merrillite. Monetite and brushite are commonly formed by precipitation from acidic, phosphorous-rich solutions [*Fiore and Laviano*, 1991; *Shellis et al.*, 1997], whereas merrillite is an igneous phosphate, actually the most common phosphatic mineral found in the SNC meteorites [*McSween and Treiman*, 1998]. Because there is not a great deal of variability in the P_2O_5: CaO ratio of these mineral phases, it is difficult to unequivocally identify the phosphate mineral present in these rocks. It is clear, however, that the differences in chemistry between brushed and RATted rock surfaces require the removal of a phosphate mineral with a higher P_2O_5: CaO ratio than apatite, which is the most common phosphate mineral encountered on Earth [*Kohn et al.*, 2002].

There is little data available for the dissolution kinetics of the mineral phases monetite, brushite, or merrilite. Tang et al. [2003] report that brushite dissolution at pH 5.5 and 37^{o}C is approximately 3-4 orders magnitude faster than that of apatite. Guidry and Mackenzie [2003] report a log dissolution rate for igneous fluorapatite at pH 2 and 25^{o}C of -10.91 mol$\cdot$m$^{-2}\cdot$s^{-1}, which is faster than that of olivine at the same conditions (see Fig. 5). We generalize on the basis of these limited dissolution rate data that phosphatic

minerals may tend to dissolve more rapidly at low pH than olivine. If this is indeed the case, then it is perhaps not surprising that a phosphatic mineral present in as large quantities as indicated for the Husband Hill Wishstone and Cumberland Ridge Watchtower type rocks would dominate the surface dissolution behavior of these rocks, even in the presence of olivine, which constitutes between ~5-20% of the Mössbauer component area of these rocks [*Klingelhöfer*, 2004; *Morris et al.*, 2005].

Soil Addition to Rock Surfaces: The "Surface", "Brushed", and "RATted" analyses of Champagne are plotted on Figure 10. For the rocks Wishstone and Watchtower no surface APXS analysis was collected, and so these rocks are not plotted on Figure 10. As shown, the position of the surface analysis of Champagne is consistent with a 2-component mixture between the brushed (altered) surface of the Champagne rock and Gusev soil. The surface analysis of Champagne is inconsistent with a 2-component mixture between the RATted (interior) of Champagne and Gusev soil.

The Champagne sample illustrates another process which may be influencing APXS analyses of rock surfaces: the addition of soil and/or dust to altered rock surfaces. The West Spur Clovis type rock Ebenezer shows sample to sample variations consistent with those demonstrated by Champagne, though mixing between soils and the RATted interior of this rock cannot be unequivocally ruled out on the basis of the relationships shown on Figure 10. For the remaining rock samples discussed (Adirondack, Humphrey, Clovis) the RATted, brushed, and surface analyses all plot within the field of Martian soils, making distinction between soil addition to brushed surfaces versus RATted surfaces difficult.

In order to further ascertain the extent to which surface APXS analyses of rocks are affected by soil addition, the surface, brushed and RATted analyses of Adirondack and Wishstone have been plotted on Figure 11A, and Humphrey, Clovis, and Ebenezer have been plotted on Figure 11B. Figures 11A and 11B are ternary diagrams which plot the mole fractions of CaO + MgO, SO_3, and Al_2O_3 at their apices. On these diagrams, the mineral dissolution relationships discussed previously result in trends directed away from the CaO+MgO apex, towards the Al_2O_3 axis. Addition of sulfate results in trends directed toward the SO_3 apex.

The rocks Wishstone and Adirondack (Fig. 11A) clearly demonstrate that the surface analyses of these rocks are consistent with 2-component mixtures between the brushed rock surface and Gusev soils. Furthermore, extrapolated tie lines between the RATted and brushed surfaces of these rocks do not terminate in the field defined by Gusev soils, indicating that the brushed surfaces are not 2-component mixtures between RATted rock and Gusev soil. Instead, the depletion in CaO and MgO is consistent with the mineral dissolution relationships discussed previously. On Figure 11B, the rocks Humphrey and Clovis demonstrate surface – brushed – RATted rock relationships consistent with those shown for Adirondack and Wishstone, however, neither the Humphrey nor Clovis surface analyses appear to be as strongly affected by soil addition as the Adirondack and Wishstone surface analyses. Finally, for the Ebenezer analyses the processes of mineral dissolution at the rock surface and soil addition to the rock surface cannot be distinguished from one another since vectors from the RATted rock interior through either the brushed analysis or the surface analysis go through the field defined by Gusev soils.

Figures 11A and 11B confirm that mineral dissolution at the rock surface, rather than soil addition to the rock surface, controls the differences in chemistry between RATted and brushed rock analyses. This is well demonstrated by analyses for the Plains Adirondack basalts, Clovis, and Wishstone. The process of soil addition to brushed rock surfaces appears to influence the chemistry of APXS surface analyses to a variable degree, with Adirondack and Wishstone surface analyses strongly influenced, and Humphrey and Clovis surface analyses less so. For the rock Ebenezer, the processes of mineral dissolution and soil addition cannot be distinguished unambiguously on Figure 10 or 11B, but the trends for this rock are entirely consistent with the processes described for the other rock samples. We note that the mineral dissolution and soil addition relationships discussed may have important implications for the understanding of Pathfinder rock chemistry, which have been interpreted as possibly representing a mixture between unaltered igneous rock and Martian soil [*Foley et al.*, 2003; *McSween et al.*, 1999].

A Model for the Formation of Rock Surface Alteration Rinds: Shown on Figure 12A-E is a schematic illustration of a potential formation pathway for alteration rinds on rock surfaces. This model applies to the mineral dissolution and soil addition relationships discussed for the Plains Adirondack, West Spur Clovis, Husband Hill Wishstone and Cumberland Ridge Watchtower type rocks. We emphasize that the leaching process discussed herein is a rock surface alteration effect which may be superimposed on an earlier stage of alteration (particularly for the West Spur Clovis type rocks, see Ming et al. [2005] and Morris et al. [2005]).

In the model, small volumes of low-pH fluids contact the rock initiating mineral dissolution at the rock surface (Fig. 12A). Since the observed alteration appears to be more extensive on the outer surfaces of rocks compared to rock interiors for both in-place outcrops and loose, non-outcrop rocks, we suggest that these fluids are deposited as either (1) an acidic aerosol (so-called "acid fog") of the type proposed by Banin et al. [1997] and Settle [1979], or (2) that they may be present as thin films of water beneath snow or frost [*Arvidson et al.*, 2004], with the fluids being acidified by dissolution of previously precipitated sulfate salts present at the rock surface [e.g., *Frau*, 2000].

In accord with the previously discussed experimental results, the chemistry of the fluid in contact with the rock surface is dominated by the elements present in the mineral phase most susceptible to acid attack (Fig. 12B). This susceptibility is determined primarily by the relative dissolution rates of the mineral phases present at the rock surface (see Fig. 5). As a result of the dissolution process, a leached alteration rind is left behind which is depleted in the elements present in the mineral phase(s) which underwent the most rapid dissolution (Fig. 12C). The fluid at the rock surface then undergoes evaporation (either while still acidified, or at higher pH depending on how much H^+ has been consumed by the dissolution process), leaving behind the secondary mineral phases formed during alteration and evaporation (Fig 12D). Vugs, pits and cracks near the rock surface have been observed in MI images of the "Plains Adirondack" type basalts to be filled with a bright material [*Arvidson et al.*, 2005; *Herkenhoff et al.*, 2004], possibly the secondary phases formed during alteration and evaporation.

In the final step, a soil/dust coating is added to the rock surface on top of the alteration rind (Fig 12E), possibly as a result of settling onto the rock surface as a result

of aeolian processes. If the soil/dust coating is cemented against the rock surface, then the soil addition process may be enhanced by transient burial of altered rocks by migrating aeolian bedforms. These bedforms could cover the rock [*Greeley et al.*, 2004], and allow for upward migration of sulfate-rich fluids (such as the type which formed the sulfate salts present in the Big Hole and Boroughs trenches, e.g. Wang et al. [2005]) cementing soil/dust adjacent to the rock into place on its surface. Such transient burial events are consistent with the observation that rocks at Gusev tend to have a heavier soil coating lower on their faces (so-called "two-toned" rocks), and that, from a geochemical standpoint, the soil coating appears to be variable from rock to rock (Fig.s 11A and 11B). Subsequent aeolian abrasion may act to remove some of the lightly cemented dust coating, secondary alteration phases, and perhaps some portion of the leached layer as well.

This model enables one to place APXS rock analyses in context, as shown in Figure 12E. The rocks analyzed by the APXS are variably coated with soil/dust, which influences the chemistry of the APXS "Surface" such that these analyses appear to be consistent with a mixture between the soil/dust coating and the underlying alteration rind. The RAT brushing operation then removes the adhering soil/dust coating from the rock surface, exposing the surface immediately beneath for the APXS "Brush" analysis. In this case, the analysis is dominated by the chemistry of the leached alteration zone, produced during interaction between acidic fluids and the rock surface. The "Brush" analysis may also be variably influenced by underlying material such as unaltered rock and/or secondary minerals, and by any soil and/or dust which has not been effectively removed by the RAT brushing operation. Finally, the RAT grinding operation produces

a circular hole in the rock face ~45mm in diameter, and ~5mm deep, and the APXS is placed against the hole for an analysis of the rock interior. The APXS RATted analysis is dominated by the chemistry of the rock interior, which lies beneath the surface alteration rind. The RATted analysis may also be affected by both alteration zone chemistry (depending on the thickness of the leached zone relative to the depth of the RAT operation), any secondary minerals in the APXS field of view, and any soil/dust/RAT cuttings which have fallen into the RAT hole.

The relationships shown on Figures 11A and 11B further suggest that the "Brushed" analyses may not be perfectly representative of a leached surface, and that the "RATted" analyses may not be perfectly representative of the rock interior. If the chemistry of RATted rock interiors and brushed rock surfaces differed only by the dissolution of mineral phases at the rock surface, then they would be expected to plot along the CaO+MgO to Al_2O_3 join on Figures 11A and 11B, since dissolution of olivine, pyroxene and Ca-phosphate only removes the soluble elements MgO and CaO without adding SO_3. This effect is demonstrated by the large arrowheads along the base of both figures. Instead, all of the analyses including RATted rock interiors have variable amounts of SO_3, indicating that there are either sulfate minerals present from the rock surface to the base of the RAT hole (e.g., in veins, which are visible in some MI images), and/or that soil contamination has affected all of the analyses from the rock surface to the base of the RAT-hole to variable degrees.

It is difficult to place meaningful constraints on the age at which the rock surfaces were altered. For the Plains Adirondack basalts, the age of emplacement of the cratered volcanic plains which constitute the floor of Gusev crater at Columbia Memorial Station

provides an upper limit on the age of alteration. On the basis of crater counts, these basalt flows are late Hesperian to early Amazonian (~3.0 Ga) in age [*Kuzmin et al.*, 2000]. However, since it appears that the alteration of these rocks is a surface effect, it seems more plausible that alteration occurred after these rocks had been broken into boulder form as a result of impact into a pre-existing lava flow. If the alteration occurred subsequent to impact into a pre-existing lava flow, alteration could have occurred at anytime subsequent to ~3.0 Ga. For rocks encountered in the Columbia Hills, the age of surface alteration could be older than ~3.0 Ga, since the emplacement of the volcanic plains post-dates that of the Columbia Hills [*Arvidson et al.*, 2005]. A key question with regards to the model shown in Fig.12 is: what is the source of the acidic fluid under the current dry climate regime? Mars is known to have been volcanically active as recently as ~165Ma [*Nyquist et al.*, 2001], and it has been suggested that during periods of persistent volcanism SO_2 gas could become globally distributed on short timescales (days), be oxidized to form sulfuric acid aerosol droplets ($H_2SO_4 \cdot nH_2O$) within months to a few years, and then gravitationally settle onto the surface within months to a few years [*Settle*, 1979]. Mars' axial obliquity is thought to have varied on the order of 0-60^o in the past few million years [*Jakosky and Phillips*, 2001], and modeling results suggest that at 35^o obliquity (currently 25^o) frost deposit thickness at Gusev crater during southern hemisphere winter would range from ~0.5-5 mm, with higher obliquity resulting in even thicker frost deposits [*Mischna et al.*, 2003]. Thus, while there is no evidence to suggest that there is currently a sulfuric acid aerosol component in the martian atmosphere, or significant frost deposition at Gusev crater, there is ample evidence to suggest that conditions have been appropriate for either, or both, of the acid sources suggested earlier

to have been present in the geologically recent past. The main point is that the rock surface leaching processes discussed herein have not been extensive for any of the lithologies discussed, and rock surface-acid interactions appear to have taken place at low fluid to rock ratio. This indicates that whenever the surface alteration took place, it did so in a relatively dry environment, which has been the defining characteristic of Gusev Crater since at least the late Hesperian to early Amazonian [*Golombek et al.*, in review; *Golombek et al.*, 2005].

Martian Soil Chemistry: Plotted on Figure 13 are the soil analyses from the Spirit, Opportunity, Pathfinder and Viking 1 landing sites. As indicated, the soil analyses from all of the sites align along a trend consistent with the experimental olivine-bearing basalt dissolution trend shown on Figure 4, and the Plains Adirondack basalt alteration trend shown on Figure 6. Based on this alignment one could interpret that the Martian soils represent a basaltic regolith which has undergone alteration at low-pH and low fluid to rock ratio resulting in chemical fractionation dominated by olivine dissolution. In such a situation, more highly altered regolith samples would plot further along the olivine dissolution trend than less altered regolith samples.

The process of alteration under the sulfuric acid dominated, low water-rock ratio, and evaporative conditions implicated for Plains Adirondack rock surfaces results primarily in the release of Mg^{2+}, Fe^{2+} and SiO_2 (aq) to solution via the rapid dissolution of olivine. Ultimately, release of these elements to solution can result in the formation of Mg-sulfates, Fe-sulfates and/or Fe-oxides, and amorphous silica. On Figure 13, the formation of Fe and Mg sulfates, as well as Fe-oxides, will result in a trend opposite to

that of olivine dissolution. Therefore, samples more enriched in sulfates and/or Fe-oxides will plot closer to the FeO_T+MgO apex than less enriched samples.

These opposing relationships make it difficult on the basis of Figure 13 alone to determine what an individual soil analysis truly represents. Each analysis could be sampling an altered basaltic regolith which either resides with the secondary minerals formed during its alteration, or has been separated from its alteration products by physical processing (similar, by analogy, to a brushed rock surface). Alternatively, an individual soil analysis could be sampling an unaltered basaltic regolith which has been physically mixed with the secondary phases formed by alteration of basaltic materials from another location. What can be said with certainty about the relationships shown on Figure 13 is that the alignment of the soil data is consistent with olivine-bearing basalt alteration as an important control on the general geochemical characteristics of Martian soils. The alignment of these data requires that they be affected principally by mobility of FeO and MgO, which can be easily generated by alteration of olivine-bearing basalt at low-pH and subsequent precipitation of FeO and MgO bearing secondary minerals.

Taken together, the soils from 4 widely separated landing sites at the Martian surface do not indicate elemental fractionation patterns consistent with alteration under conditions similar to those on Earth. This can be seen by comparison to the terrestrial alteration trends shown on Figure 13. On a global scale, this implies that the alteration processes occurring in the surface environment on Mars are largely characterized by interactions between low-pH fluids and basaltic rock/regolith at low water to rock ratio, analogous to the alteration process occurring at the microscopic scale on the surfaces of the Plains Adirondack basalts. If the soil forming process on Mars were similar to that

occurring at the moderate pH and high water to rock ratio conditions endemic to planet Earth, one would expect to see chemical fractionations significantly more like those observed for terrestrial weathering profiles.

It is interesting to note that if weathering via interaction with acidic fluids is a globally important control on the geochemistry of soils and rocks in the Martian surface environment, then carbonate minerals are not likely to be present in these deposits. Siderite ($FeCO_3$), the least soluble of the carbonate minerals, precipitates only at pH values greater than about 5, while calcite ($CaCO_3$) and magnesite ($MgCO_3$) are even more soluble [*Catling*, 1999]. Carbonate minerals would not be expected to precipitate under the acidic soil/rock alteration regime implicated herein, and any pre-existing carbonates would be expected to dissolve during interaction with such fluids [*Falren et al.*, 2004].

Conclusions: The effects of alteration at low pH produce fundamentally different major element relationships from those observed for alteration under typical conditions on Earth. This is the result of the fact that at low pH, Al and Fe (III) are far more soluble, and the oxidation rate of Fe (II) to less soluble Fe (III) is far lower, than in the pH range of natural waters on Earth. In effect, the elements commonly taken to be immobile in terrestrial weathering profiles (Al and Fe) are mobile in the low-pH environment. Chemical fractionations observed during experimental low-pH (=0-1) alteration of synthetic Martian basalts reveal that solution chemistry is dominated by mineral dissolution, rather than the alkali and alkaline earth element leaching associated with alteration of feldspar and other silicate minerals that is observed for moderate pH (=5-9)

weathering on Earth. The experimental data further indicate that the contribution each mineral phase makes to the solution composition is determined by their relative dissolution rates.

Application of experimental results to understanding the chemistry of the surfaces of rocks exposed on the Gusev Plains and Columbia Hills indicates that the differences in chemical composition between Brushed and RATted rock analyses can be explained by low-pH mineral phase dissolution resulting from interactions between small volumes of acidic fluid and rock surfaces. In the case of the Plains Adirondack type basalts, olivine dissolution is indicated, the West Spur Clovis type rocks may indicate pyroxene and/or basaltic glass dissolution, and the Husband Hill Wishstone and Cumberland Ridge Watchtower type rocks indicate Ca-phosphate dissolution. In all cases, the observed differences in chemical composition are in good agreement with the dissolution behavior one would predict on the basis of relative dissolution rates and experimental data on basalt alteration at low pH. Furthermore, using the mass lost during experimental alteration of olivine-bearing basalts as a constraint, the mineral dissolution processes evident at the surfaces of Plains Adirondack type basalts may have occurred at fluid to rock ratios <10. By inference, the same may be true of the other rock surfaces discussed in this paper.

The geochemistry of pristine rock surfaces can be best described as a mixture between variable amounts of adhering soil and a leached alteration rind immediately beneath the soil veneer. APXS analyses of brushed rock surfaces are dominated by the geochemistry of a leached alteration rind produced by low fluid to rock ratio interactions between rock surfaces and acidic fluids. The geochemistry of RATted rock surfaces

appears to be relatively unaffected by these surface leaching interactions, and so the APXS RATted analyses predominantly carry the signature of rock interiors.

A significant part of the chemical variation observed in Martian soils can be said to be consistent with alteration similar to that observed for the Plains Adirondack basalts, which is strongly influenced by the dissolution of olivine and the formation of secondary Mg (±Fe) sulfates and Fe-oxides. In general, rock alteration profiles analyzed at Gusev crater, and soils analyzed at the Spirit, Opportunity, Pathfinder and Viking 1 landing sites do not mimic the chemical fractionations produced by basalt alteration on Earth, indicating they have not been altered by interaction with large volumes of moderate pH water.

Acknowledgements: We are grateful to the entire science and engineering teams on MER who made this investigation possible. JAH and NJT are also indebted to the members of the Soil and Rock Physical Properties theme group who involved us in the fascinating data returns from soil and rock analyses at Gusev Crater from day one of our participation in the MER science team. The MER project is funded by the National Aeronautics and Space Administration. This work was also partially supported by NASA Cosmochemistry Program grant NAG5-12916 to S.M.M.

References:

Arvidson, R., S. Squyres, R. Anderson, J. Bell III, J. Brückner, N. Cabrol, W. Calvin, M. Carr, P. Christensen, B. Clark, L. Crumpler, D. DesMarais, C. d'Uston, T. Economou, J. Farmer, W. Farrand, W. Folkner, M. Golombek, S. Gorevan, J. Grant, R. Greeley, J. Grotzinger, E. Guinness, B. Hahn, L. Haskin, K. Herkenhoff, J. Hurowitz, S. Hviid, J. Johnson, G. Klingelhöfer, A. Knoll, G. Landis, C. Leff, M. Lemmon, R. Li, M. Madsen, M. Malin, S. McLennan, H. McSween, D. Ming, J. Moersch, R. Morris, T. Parker, J. Rice Jr., L. Richter, R. Rieder, M. Sims, M. Smith, P. Smith, L. Soderblom, R. Sullivan, N. Tosca, H. Wänke, J. Ward, T. Wdowiak, M. Wolff, and A. Yen, Overview of the Spirit Mars Exploration Rover mission to Gusev Crater: Landing site to the Methuselah outcrop in the Columbia Hills, *Journal of Geophysical Research* (this issue), 2005.

Arvidson, R.E., R.C. Anderson, P. Bartlett, J.F. Bell, III, D. Blaney, P.R. Christensen, P. Chu, L. Crumpler, K. Davis, B.L. Ehlmann, R. Fergason, M.P. Golombek, S. Gorevan, J.A. Grant, R. Greeley, E.A. Guinness, A.F.C. Haldemann, K. Herkenhoff, J. Johnson, G. Landis, R. Li, R. Lindemann, H. McSween, D.W. Ming, T. Myrick, L. Richter, F.P. Seelos, IV, S.W. Squyres, R.J. Sullivan, A. Wang, and J. Wilson, Localization and Physical Properties Experiments Conducted by Spirit at Gusev Crater, *Science*, *305* (5685), 821-824, 2004.

Banin, A., H. Kan, and A. Cicelsky, Acidic volatiles and the Mars soil, *Journal of Geophysical Research*, *102* (E6), 13341-13356, 1997.

Blum, A., and L. Stillings, Feldspar Dissolution Kinetics, in *Chemical Weathering Rates of Silicate Minerals*, edited by A. White, and S. Brantley, pp. 291-352, Mineralogical Society of America, Washington, DC, 1995.

Brantley, S., and Y. Chen, Chemical Weathering Rates of Pyroxenes and Amphiboles, in *Chemical Weathering Rates of Silicate Minerals*, edited by A. White, and S. Brantley, pp. 119-172, Mineralogical Society of America, Washington, DC, 1995.

Burns, R., Rates and mechanisms of chemical weathering of ferromagnesian silicate minerals on Mars, *Geochimica et Cosmochimica Acta*, *57*, 4555-4574, 1993.

Burns, R., and D. Fisher, Rates of oxidative weathering on the surface of Mars, *Journal of Geophysical Research*, *98* (E2), 3365-3372, 1993.

Burns, R.G., Ferric Sulfates on Mars, *Journal of Geophysical Research-Solid Earth and Planets*, *92* (B4), E570-E574, 1987.

Catling, D., A chemical model for evaporites on early Mars: possible sedimentary tracers of the early climate and implications for exploration, *Journal of Geophysical Research*, *104* (E7), 16453-16469, 1999.

Clark, B., A. Baird, R. Weldon, D. Tsusaki, L. Schnabel, and M. Candelaria, Chemical composition of Martian fines, *Journal of Geophysical Research*, *105*, 9623-9642, 1982.

Clark, B., and D. Van Hart, The salts of Mars, *Icarus*, *45* (2), 370-378, 1981.

Delany, J., and S. Lundeen, The LLNL thermochemical database, pp. 150, Lawrence Livermore National Laboratory, 1990.

Eggleton, R., C. Foudoulis, and V. D, Weathering of basalt: Changes in rock chemistry and mineralogy, *Clay and Clay Minerals*, *35*, 161-169, 1987.

Falren, A., D. Fernandez-Remolar, J. Dohm, V. Baker, and R. Amils, Inhibition of carbonate synthesis in acidic oceans on early Mars, *Nature*, *431*, 423-426, 2004.

Fedo, C., H. Nesbitt, and G. Young, Unraveling the effects of potassium metasomatism in sedimentary rocks and paleosols, with implications for paleoweathering conditions and provenance, *Geology*, *23* (10), 921-924, 1995.

Fiore, S., and R. Laviano, Brushite, Hydroxylapatite, and Taranakite from Apulian Caves (Southern Italy) - New Mineralogical Data, *American Mineralogist*, *76* (9-10), 1722-1727, 1991.

Foley, C., T. Economou, and R. Clayton, Final chemical results from the Mars Pathfinder alpha proton X-ray spectrometer, *Journal of Geophysical Research*, *108* (E12), 8096, doi: 10.1029/2002JE002019, 2003.

Frau, F., The formation-dissolution-precipitation cycle of melanterite at the abandoned pyrite mine of Genna Luas in Sardinia, Italy: environmental implications, *Mineralogical Magazine*, *64* (6), 995-1006, 2000.

Gellert, R., R. Rieder, R.C. Anderson, J. Bruckner, B.C. Clark, G. Dreibus, T. Economou, G. Klingelhöfer, G.W. Lugmair, D.W. Ming, S.W. Squyres, C. d'Uston, H. Wanke, A. Yen, and J. Zipfel, Chemistry of Rocks and Soils in Gusev Crater from the Alpha Particle X-ray Spectrometer, *Science*, *305* (5685), 829-832, 2004.

Gellert, R., R. Rieder, J. Brückner, B. Clark, G. Dreibus, G. Lugmair, D. Ming, H. Wanke, A. Yen, and J. Zipfel, The Alpha Particle X-Ray Spectrometer (APXS): Results from Gusev Crater and calibration report, *Journal of Geophysical Research* (this issue), 2005.

Gislason, S., and S. Arnorsson, Dissolution of primary basaltic minerals in natural-waters-saturation state and kinetics, *Chemical Geology*, *105* (1-3), 117-135, 1993.

Gislason, S., and O. Eugster, Meteoric water-basalt interactions. II: A field study in N.E. Iceland, *Geochimica et Cosmochimica Acta*, *51*, 2841-2855, 1987.

Gislason, S.R., S. Arnorsson, and H. Armannsson, Chemical weathering of basalt in southwest Iceland: Effects of runoff, age of rocks and vegetative/glacial cover, *American Journal of Science*, *296* (8), 837-907, 1996.

Golombek, M., J. Grant, L. Crumpler, R. Greeley, R. Arvidson, P. Christensen, J. Bell III, and S. Squyres, Climate change from the Mars Exploration Rover landing sites: From wet in the Noachian to dry and dessicating since the Hesperian, *Nature*, in review.

Golombek, M., J. Grant, L. Crumpler, R. Greeley, R. Arvidson, and the Athena Science Team, Climate change from the Mars Exploration Rover landing sites: From wet in the Noachian to dry and dessicating since the Hesperian, in *Lunar and Planetary Science 36, Abstract #1539*, Houston (CD-ROM), 2005.

Gorevan, S., T. Myrick, K. Davis, J. Chau, P. Bartlett, S. Mukherjee, S. Stroescu, C. Batting, R. Andersen, and S. Squyres, The Rock Abrasion Tool, Mars Exploration Rover Mission, *Journal of Geophysical Research* (this issue), 2005.

Gorevan, S.P., T. Myrick, K. Davis, J.J. Chau, P. Bartlett, S. Mukherjee, R. Anderson, S.W. Squyres, R.E. Arvidson, M.B. Madsen, P. Bertelsen, W. Goetz, C.S. Binau, and L. Richter, Rock Abrasion Tool: Mars exploration Rover mission, *Journal of Geophysical Research-Planets*, *108* (E12), 2003.

Greeley, R., S.W. Squyres, R.E. Arvidson, P. Bartlett, J.F. Bell, III, D. Blaney, N.A. Cabrol, J. Farmer, B. Farrand, M.P. Golombek, S.P. Gorevan, J.A. Grant, A.F.C.

Haldemann, K.E. Herkenhoff, J. Johnson, G. Landis, M.B. Madsen, S.M. McLennan, J. Moersch, J.W. Rice, Jr., L. Richter, S. Ruff, R.J. Sullivan, S.D. Thompson, A. Wang, C.M. Weitz, and P. Whelley, Wind-Related Processes Detected by the Spirit Rover at Gusev Crater, Mars, *Science*, *305* (5685), 810-813, 2004.

Guidry, M., and F. Mackenzie, Experimental study of igneous and sedimentary apatite dissolution: Control of pH, distance from equilibrium, and temperature on dissolution rates, *Geochimica et Cosmochimica Acta*, *67* (16), 2949-2963, 2003.

Haskin, L., A. Wang, H. McSween, S. McLennan, N. Cabrol, L. Crumpler, B. Jolliff, A. Yen, B. Clark, D. DesMarais, S. Squyres, R. Arvidson, D. Ming, R. Morris, N. Tosca, J. Hurowitz, R. Gellert, G. Klingelhöfer, J. Bell III, K. Herkenhoff, P. Christensen, S. Ruff, D. Blaney, J. Farmer, J. Grant, R. Greeley, E. Grin, G. Landis, J. Rice, L. Richter, C. Schröder, L. Soderblom, and P. de Souza Jr., Water alteration of rocks and soils from the Spirit rover site, Gusev Crater, Mars, *Nature*, in press.

Herkenhoff, K.E., S.W. Squyres, R. Arvidson, D.S. Bass, J.F. Bell, III, P. Bertelsen, N.A. Cabrol, L. Gaddis, A.G. Hayes, S.F. Hviid, J.R. Johnson, K.M. Kinch, M.B. Madsen, J.N. Maki, S.M. McLennan, H.Y. McSween, J.W. Rice, Jr., M. Sims, P.H. Smith, L.A. Soderblom, N. Spanovich, R. Sullivan, and A. Wang, Textures of the Soils and Rocks at Gusev Crater from Spirit's Microscopic Imager, *Science*, *305* (5685), 824-826, 2004.

Hurowitz, J., S. McLennan, D. Lindsley, and M. Schoonen, Experimental epithermal alteration of synthetic Los Angeles meteorite: Implications for the origin of Martian soils and identification of hydrothermal sites on Mars, *Journal of Geophysical Research*, in press.

Jakosky, B., and R. Phillips, Mars' volatile and climate history, *Nature*, *412*, 237-244, 2001.

Karrat, L., A. Perruchot, and J. Macaire, Weathering of a Quaternary glass-rich basalt in Bakrit, Middle Atlas Mountains, Morocco. Comparison with a glass-poor basalt, *Geodinamica Acta*, *11* (5), 205-215, 1998.

Klingelhöfer, G., MER 1 Mössbauer 1 EDR V1.0, NASA Planetary Data System, MER1-M-MB-1-EDR-OPS-V1.0, 2004.

Klingelhöfer, G., R. Morris, B. Bernhardt, D. Rodionov, P.J. de Souza, S. Squyres, J. Foh, U. Bonnes, R. Gellert, C. Schröder, S. Linkin, E. Evlanov, B. Zubcov, and O. Prilutski, Athena MIMOS II Mössbauer spectrometer investigation, *Journal of Geophysical Research*, *108* (E12), doi:10.1029/2003JE002138, 2003.

Klingelhöfer, G., R.V. Morris, B. Bernhardt, C. Schröder, D.S. Rodionov, P.A. de Souza, Jr., A. Yen, R. Gellert, E.N. Evlanov, B. Zubkov, J. Foh, U. Bonnes, E. Kankeleit, P. Gutlich, D.W. Ming, F. Renz, T. Wdowiak, S.W. Squyres, and R.E. Arvidson, Jarosite and Hematite at Meridiani Planum from Opportunity's Mössbauer Spectrometer, *Science*, *306* (5702), 1740-1745, 2004.

Kohn, M., J. Rakovan, and J. Hughes, Phosphates - Geochemical, Geobiological, and Materials Importance, in *Reviews in Mineralogy and Geochemistry*, edited by P. Ribbe, Mineralogical Society of America, Washington, D.C., 2002.

Kuzmin, R., R. Greeley, R. Landheim, N. Cabrol, and J. Farmer, Geologic map of the MTM-15182 and MTM-15187 quadrangles, Gusev Crater-Ma'adim Vallis region, Mars, U.S. Geological Survey, 2000.

McLennan, S., Relationships between the trace element composition of sedimentary rocks and upper continental crust, *G*^{3}, *2*, 2000GC000109, 2001.

McLennan, S., S. Hemming, D. McDaniel, and G. Hanson, Geochemical approaches to sedimentation, provenance and tectonics, in *Processes Controlling the Composition of Clastic Sediments*, edited by M. Johnsson, and A. Basu, pp. 21-40, Geological Society of America Special Paper, Boulder, 1993.

McSween, H., R. Arvidson, J. Bell III, D. Blaney, N. Cabrol, P. Christensen, B. Clark, J. Crisp, L. Crumpler, D. DesMarais, J. Farmer, R. Gellert, A. Ghosh, S. Gorevan, T. Graff, J. Grant, L. Haskin, K. Herkenhoff, J. Johnson, B. Jolliff, G. Klingelhöfer, A. Knudsen, S. McLennan, K. Milam, J. Moersh, R. Morris, R. Rieder, S. Ruff, P.J. de Souza, S. Squyres, H. Wanke, A. Wang, M. Wyatt, A. Yen, and J. Zipfel, Basaltic rocks analyzed by the Spirit rover in Gusev Crater, *Science*, *305* (5685), 842-845, 2004.

McSween, H., T. Grove, and M. Wyatt, Constraints on the composition and petrogenesis of the Martian crust, *Journal of Geophysical Research-Planets*, *108* (E12), 2003.

McSween, H., and K. Keil, Mixing relationships in the Martian regolith and the composition of globally homogeneous dust, *Geochimica et Cosmochimica Acta*, *64* (12), 2155-2166, 2000.

McSween, H., S. Murchie, J. Crisp, N. Bridges, R. Anderson, J. Bell III, D. Britt, G. Dreibus, T. Economou, A. Ghosh, M. Golombek, J. Greenwood, J. Johnson, H. Moore, R. Morris, T. Parker, R. Rieder, R. Singer, and H. Wanke, Chemical, multispectral, and textural constraints on the composition and origin of rocks at the Mars Pathfinder landing site, *Journal of Geophysical Research*, *104* (E4), 8679-8715, 1999.

McSween, H., and A. Treiman, Martian Meteorites, in *Planetary Materials*, edited by J. Papike, Mineralogical Society of America, Washington, D.C., 1998.

Meyer, C., Mars Meteorite Compendium, Astromaterials Research & Exploration Science (ARES), Lyndon B. Johnson Space Center, Houston, 2004.

Michalski, J., M. Kraft, T. Sharp, and P. Christensen, Palagonite-like alteration products on the Earth and Mars I: Spectroscopy (0.4-25 microns) of weathered basalts and silicate alteration products, in *Lunar and Planetary Science 36, Abstract #1188*, Houston (CD-ROM), 2005a.

Michalski, J., M. Kraft, T. Sharp, L. Williams, and P. Christensen, Mineralogical constraints on the high-silica Martian surface component observed by TES: clay-rich mineralogy does not sufficiently explain the Acidalia Planitia-type spectra, *Icarus*, *174* (1), 161-177, 2005b.

Ming, D., et al., Geochemical and mineralogical indicators for aqueous processes in the Columbia Hills of Gusev Crater, Mars, *Journal of Geophysical Research* (this issue), 2005.

Mischna, M., M. Richardson, R. Wilson, and D. McCleese, On the orbital forcing of Martian water and CO_2 cycles: A general circulation model study with simplified volatile schemes, *Journal of Geophysical Research*, *108* (E6), doi: 10.1029/2003JE002051, 2003, 2003.

Morris, R., D. Golden, J. Bell III, T. Shelfer, A. Scheinost, N. Hinman, G. Furniss, S. Mertzman, J. Bishop, D. Ming, C. Allen, and D. Britt, Mineralogy, composition and alteration of Mars Pathfinder rocks and soils: evidence from multispectral, elemental and magnetic data on terrestrial analogue, SNC meteorite, and Pathfinder samples, *Journal of Geophysical Research*, *105* (E1), 1757-1817, 2000.

Morris, R., G. Klingelhöfer, C. Schröder, and D. Rodionov, et al., Mössbauer mineralogy of rock and soil at Gusev Crater: Spirit's journey through weakly altered olivine basalt on the Gusev Plains and pervasively altered basalt in the Columbia Hills, *Journal of Geophysical Research* (this issue), 2005.

Morris, R.V., G. Klingelhöfer, B. Bernhardt, C. Schröder, D.S. Rodionov, P.A. de Souza, Jr., A. Yen, R. Gellert, E.N. Evlanov, J. Foh, E. Kankeleit, P. Gutlich, D.W. Ming, F. Renz, T. Wdowiak, S.W. Squyres, and R.E. Arvidson, Mineralogy at Gusev Crater from the Mössbauer Spectrometer on the Spirit Rover, *Science*, *305* (5685), 833-836, 2004.

Nesbitt, H., and G. Markovics, Weathering of granodioritic crust, long-term storage of elements in weathering profiles, and petrogenesis of siliciclastic sediments, *Geochimica et Cosmochimica Acta*, *61* (8), 1653-1670, 1997.

Nesbitt, H., and R. Wilson, Recent chemical weathering of basalts, *American Journal of Science*, *292*, 740-777, 1992.

Nesbitt, H., and G. Young, Early Proterozoic climates and plate motions inferred from major element chemistry of lutites, *Nature*, *299*, 715-717, 1982.

Nesbitt, H., and G. Young, Prediction of some weathering trends of plutonic and volcanic rocks based on thermodynamic and kinetic considerations, *Geochimica et Cosmochimica Acta*, *48*, 1523-1534, 1984.

Nesbitt, H., G. Young, S. McLennan, and R. Keays, Effects of chemical weathering and sorting on the petrogenesis of siliciclastic sediments, with implications for provenance studies, *Journal of Geology*, *104*, 525-542, 1996.

Newsom, H., J. Hagerty, and F. Goff, Mixed hydrothermal fluids and the origin of the Martian soil, *Journal of Geophysical Research*, *104* (E4), 8717-8728, 1999.

Nyquist, L., D. Bogard, C. Shih, A. Grishake, D. Stoffler, and O. Eugster, Ages and geologic histories of martian meteorites, *Space Science Reviews*, *96*, 105-164, 2001.

Patchett, P., G. Ross, and J. Gleason, Continental drainage in North America during the Phanerozoic from Nd Isotopes, *Science*, *283*, 671-673, 1999.

Patterson, S., Investigations of ferruginous bauxite and other mineral resources on Kauai and a reconnaissance of ferruginous bauxite deposits on Maui, Hawaii, pp. 65, USGS Professional Paper 656, 1971.

Pokrovsky, O., and J. Schott, Kinetics and mechanism of forsterite dissolution at 25C and pH from 1 to 12, *Geochimica et Cosmochimica Acta*, *64* (19), 3313-3325, 2000.

Rieder, R., MER 1 Alpha Particle X-Ray Spectrometer 2 EDR V1.0, NASA Planetary Data System, MER1-M-APXS-2-EDR-OPS-V1.0, 2004.

Rieder, R., R. Gellert, R.C. Anderson, J. Bruckner, B.C. Clark, G. Dreibus, T. Economou, G. Klingelhöfer, G.W. Lugmair, D.W. Ming, S.W. Squyres, C. d'Uston, H. Wanke, A. Yen, and J. Zipfel, Chemistry of Rocks and Soils at Meridiani Planum

from the Alpha Particle X-ray Spectrometer, *Science*, *306* (5702), 1746-1749, 2004.

Rieder, R., R. Gellert, J. Bruckner, G. Klingelhöfer, G. Dreibus, A. Yen, and S.W. Squyres, The new Athena alpha particle X-ray spectrometer for the Mars Exploration Rovers, *Journal of Geophysical Research-Planets*, *108* (E12), 2003.

Ruff, S., P. Christensen, D. Blaney, W. Farrand, J. Johnson, J. Michalski, J. Moersch, and S. Wright, The rocks of Gusev Crater as viewed by the Mini-TES instrument, *Journal of Geophysical Research* (this issue), 2005.

Schröder, C., et al., Evidence for olivine weathering in rocks at Gusev crater, *Journal of Geophysical Research* (this issue), 2005.

Settle, M., Formation and deposition of volcanic sulfate aerosols on Mars, *Journal of Geophysical Research*, *84* (B14), 8343-8354, 1979.

Shellis, R., B. Heywood, and F. Wahab, Formation of brushite, monetite and whitlockite during equilibration of human enamel with acid solutions at 37 degrees C, *Caries Research*, *31* (1), 71-7, 1997.

Squyres, S., R. Arvidson, J. Bell III, P. Christensen, W. Farrand, R. Gellert, S. Gorevan, K. Herkenhoff, J. Johnson, G. Klingelhöfer, D. Ming, R. Morris, and S. Ruff, Rock and soil types of the Columbia Hills, *Journal of Geophysical Research* (this issue), 2005.

Squyres, S.W., J.P. Grotzinger, R.E. Arvidson, J.F. Bell, III, W. Calvin, P.R. Christensen, B.C. Clark, J.A. Crisp, W.H. Farrand, K.E. Herkenhoff, J.R. Johnson, G. Klingelhöfer, A.H. Knoll, S.M. McLennan, H.Y. McSween, Jr., R.V. Morris, J.W. Rice, Jr., R. Rieder, and L.A. Soderblom, In Situ Evidence for an Ancient Aqueous Environment at Meridiani Planum, Mars, *Science*, *306* (5702), 1709-1714, 2004.

Stumm, W., and J. Morgan, *Aquatic Chemistry: Chemical Equilibria and Rates in Natural Waters*, 1022 pp., John Wiley & Sons, Inc., New York, 1996.

Tang, R.K., M. Hass, W.J. Wu, S. Gulde, and G.H. Nancollas, Constant composition dissolution of mixed phases II. Selective dissolution of calcium phosphates, *Journal of Colloid and Interface Science*, *260* (2), 379-384, 2003.

Taylor, S., and S. McLennan, *The Continental Crust: its Composition and Evolution*, 312 pp., Blackwell Scientific Publications, Oxford, 1985.

Tosca, N., S. McLennan, B. Clark, J. Grotzinger, J. Hurowitz, A. Knoll, C. Schröder, and S. Squyres, Geochemical Modeling of Evaporation Processes on Mars: Insight from the Sedimentary Record at Meridiani Planum, *Earth and Planetary Science Letters*, in press.

Tosca, N., S. McLennan, D. Lindsley, and M. Schoonen, Acid-sulfate weathering of synthetic Martian basalt: The acid-fog model revisited, *Journal of Geophysical Research*, *109*, E05003, doi: 10.1029/2003JE002218, 2004.

Wang, A., L. Haskin, S. Squyres, B. Joliff, L. Crumpler, R. Gellert, C. Schröder, K. Herkenhoff, J. Hurowitz, N. Tosca, W. Farrand, and R. Anderson, Sulfate deposition in subsurface regolith in Gusev crater, Mars, *Journal of Geophysical Research* (this issue), 2005.

White, A., and S. Brantley, Chemical Weathering Rates of Silicate Minerals, in *Reviews in Mineralogy*, edited by P. Ribbe, pp. 581, Mineralogical Society of America, Washington D.C., 1995.

White, A., M. Peterson, and M. Hochella Jr., Electrochemistry and dissolution kinetics of magnetite and ilmenite, *Geochimica et Cosmochimica Acta*, *58* (8), 1859-1875, 1994.

Wogelius, R., and J. Walther, Olivine dissolution kinetics at near-surface conditions, *Chemical Geology*, *97* (1-2), 101-112, 1992.

Captions:

Figure 1: Ternary FeO_T + MgO (FM), Al_2O_3 (A), CaO + Na_2O + K_2O (CNK) diagram, data plotted in mole percent. Black triangles are the Toorongo granodiorite weathering profile; black squares are the Baynton basalt weathering profile (see text for references). Black circles are the Los Angeles, Shergotty, EETA79001A/B, QUE94201, SaU005, Zagami, and DaG476 basaltic Shergottites, data from compilation in Meyer [2004]. White diamonds are minerals, Hb=hornblende, Bi=biotite, Ch=chlorite, Sm=smectite, ill=illite, Ka/Gi=kaolinite and gibbsite, after Nesbitt and Wilson [1992].

Figure 2A-2C: **(2A)** Log activity of Al^{3+} vs. pH showing speciation of Al with respect to kaolinite precipitation. Activity of SiO_2(aq) set by assuming saturation with respect to amorphous silica, pyrophyllite precipitation suppressed. **(2B)** Log activity of Fe^{3+} vs. pH showing speciation of ferric iron with respect to goethite precipitation, hematite precipitation suppressed (**2B**). Log rate of iron oxidation (mol/L/day) vs. pH (**2C**). On all diagrams, gray field denotes the pH range of most natural terrestrial waters, cross-hatched field represents the pH range of experiments conducted by Hurowitz et al. (in press) and Tosca et al (2004). Equilibrium speciation diagrams (**Figs. 2A, 2B**) calculated at 25°C using the Lawrence Livermore National Laboratory thermochemical database [*Delany and Lundeen*, 1990]. Fe-oxidation rate vs. pH diagram (**Fig. 2C**) calculated at 25°C, pO_2 = 0.2 atm, and activity Fe^{2+} = 1 using rate equations in Stumm and Morgan [1996].

Figure 3: Ternary diagram showing the composition of the synthetic Los Angeles Shergottite basalt (LA) (black square) [*Hurowitz et al.*, in press] and calculated residue (gray square) remaining after alteration at pH = 1.0 and fluid to rock ratio = 1000. As shown, alteration is dominated by dissolution of plagioclase. Note however that the plagioclase dissolution trend does not extend to the position of plagioclase indicating that the dissolution of titanomagnetite also plays a role in determining the dissolution trend vector as well. Also shown are the terrestrial weathering trends from Fig. 1.

Figure 4: Ternary diagram showing the composition of the synthetic Pathfinder soil basalt (PFS) (black circle) [*Tosca et al.*, 2004] and calculated residue (gray circle) remaining after alteration at pH = 0 and fluid to rock ratio = 10. As shown, alteration is dominated by dissolution of olivine.

Figure 5: Log mineral dissolution rates (mol/cm^2/sec) determined experimentally at pH = 2 and 25°C. Data from [*Blum and Stillings*, 1995; *Brantley and Chen*, 1995; *Guidry and Mackenzie*, 2003; *Pokrovsky and Schott*, 2000; *White et al.*, 1994; *Wogelius and Walther*, 1992]. Arrows point to fastest dissolving mineral phases present in synthetic LA and PFS basalts [*Hurowitz et al.*, in press; *Tosca et al.*, 2004], see text for details.

Figure 6: Ternary diagram showing the composition of target Adirondack_RAT (black circle with white outline), Adirondack_brush (gray circle), Humphrey_RAT2 (black square), and Humphrey_brush (gray square). Data from Gellert et al. [2005] and Rieder [2004]. The brushed analyses are depleted in FeO_T and MgO relative to RATted analyses, indicating dissolution of olivine from the rock surfaces.

Figure 7: Ternary diagram showing the composition of target Ebenezer_RAT (black circle), Ebenezer_brushed (gray circle), Clovis_Plano_RAT (black square), and Clovis_Plano_Brush (gray square). Data from Gellert et al. [2005] and Rieder [2004]. The brushed analyses of Ebenezer and Clovis are depleted in FeO_T and MgO relative to RATted analyses, possibly indicating dissolution of pyroxene and/or basaltic glass from

the rock surfaces. Also shown are the average unaltered Hawaiitic tephra (black triangle) and solfatetic tephras (grey triangles) of Morris et al. [2000].

Figure 8: Ternary diagram showing the composition of Wishstone_Chisel_RAT (black circle with white outline), Wishstone_Chisel_brushed (gray circle), Champagne_RAT (black square), Champagne_brush (gray square), Watchtower_Joker_RAT (black triangle), and Watchtower_Joker_Brush (gray triangle). Data from Gellert et al. [2005] and Rieder [2004]. Also plotted is Na-merrillite ($Ca_{18}Na_2Mg_2(PO_4)_{14}$, white diamond). The brushed analyses are depleted in CaO relative to RATted analyses, indicating dissolution of Ca-phosphate from the rock surfaces.

Figure 9: Ternary FeO_T + MgO + Na_2O + K_2O (FMNK), P_2O_5 (P), CaO (C) diagram, data plotted in mole percent. Minerals plotted as white diamonds, formulas for apatite, carbonate apatite, Ca and Na-merrilite, brushite, and monetite are: $Ca_5(PO_4)_3(OH)_{0.33}F_{0.33}Cl_{0.33}$, $Ca_5(PO_4,CO_3)_3F$, $Ca_{19}Mg_2(PO_4)_{14}$, and $Ca_{18}Na_2Mg_2(PO_4)_{14}$, $CaHPO_4{\cdot}_2H2O$, and $CaHPO_4$, respectively. All other symbols are the same as Figure 8, data from Gellert et al. [2005] and Rieder [2004]. The solid line is an extrapolation to the CaO-P_2O_5 join of a tie line drawn between the RATted and brushed compositions of Champagne. The dashed line is drawn from the position of merrillite to the brushed composition of Champagne. It is difficult to tell which phase, brushite or merrillite, is being dissolved from the rock surface to generate the differences in chemistry between RATted and brushed analyses.

Figure 10: Ternary diagram showing the composition of Champagne_RAT (black square), Champagne_brush (gray square), Champagne_as is (white square), Ebenezer_RAT (black circle), Ebenezer_brushed (gray circle), and Ebenezer_as is (white circle). Also shown as a cross hatched field are the soil analyses from Gusev crater. Data from Gellert et al. [2005] and Rieder [2004]. The dash line is an extrapolation of a tie line between the "RATted" and "Surface" APXS analyses of Champagne demonstrating that the "Surface" analysis is not a mixture between Gusev soil and the rock interior. The pristine surfaces of Champagne and Ebenezer demonstrate the effect of soil addition to brushed rock surfaces, shown by the solid arrowhead lines.

Figure 11A-B: Ternary CaO + MgO, SO_3, Al_2O_3 diagrams, data plotted in mole percent. Only the lower right portion of the full ternary diagrams are shown, as indicated by the gray field in the "guide diagram" shown on the upper right. This is done in order to magnify the differences between analyses of different rock surfaces. Figures 11A and 11B plot all Gusev soils except subsurface soils from the "Big Hole" and "The Boroughs" trenches. The soil analysis "Paso Robles" plots off of both diagrams toward the SO_3 axis. Figure 11A plots the "Surface", "Brushed" and "RATted" analyses of Adirondack and Wishstone, Figure 11B plots the same data for Humphrey, Clovis and Ebenezer, as indicated in the legends. The dashed lines are extrapolations of tie lines between the "RATted" and "Brushed" APXS analyses. The heavy black lines are tie lines between the "Brushed" and "Surface" APXS analyses. The large arrowheads along the bases of both figures illustrate the effect of pure mineral phase dissolution with no addition of SO_3. All data from Gellert et al. [2005] and Rieder [2004].

Figure 12A-E: Schematic illustration of alteration processes occurring at rock surfaces, see text for detailed description.

Figure 13: Ternary diagram showing soil analyses from the Spirit (white circles), Opportunity (black triangles), Pathfinder (white triangles), and Viking 1 (black X's)

landing sites. Data from Gellert et al. [2005] and Rieder [2004], Reider et al. [2004], Foley et al. [2003], and Clark et al. [1982].

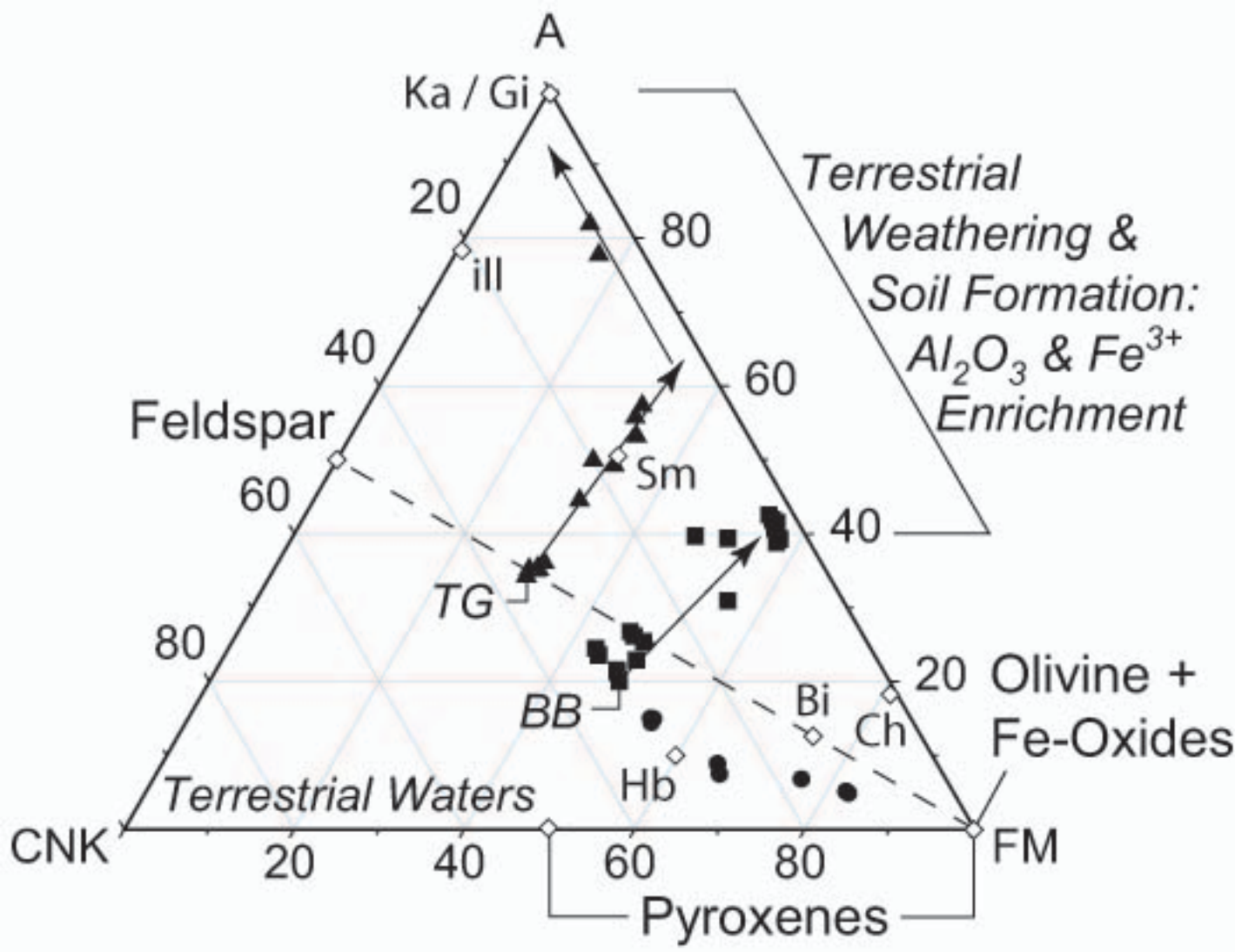
A
Ka / Gi
20
80
ill
40
60
Feldspar
Sm
60
40
TG
80
20
Olivine +
Fe-Oxides
BB
Bi
Ch
Hb
Terrestrial Waters
CNK
20
40
60
80
FM
Pyroxenes
Terrestrial
Weathering &
Soil Formation:
Al_2O_3 & Fe^{3+}
Enrichment

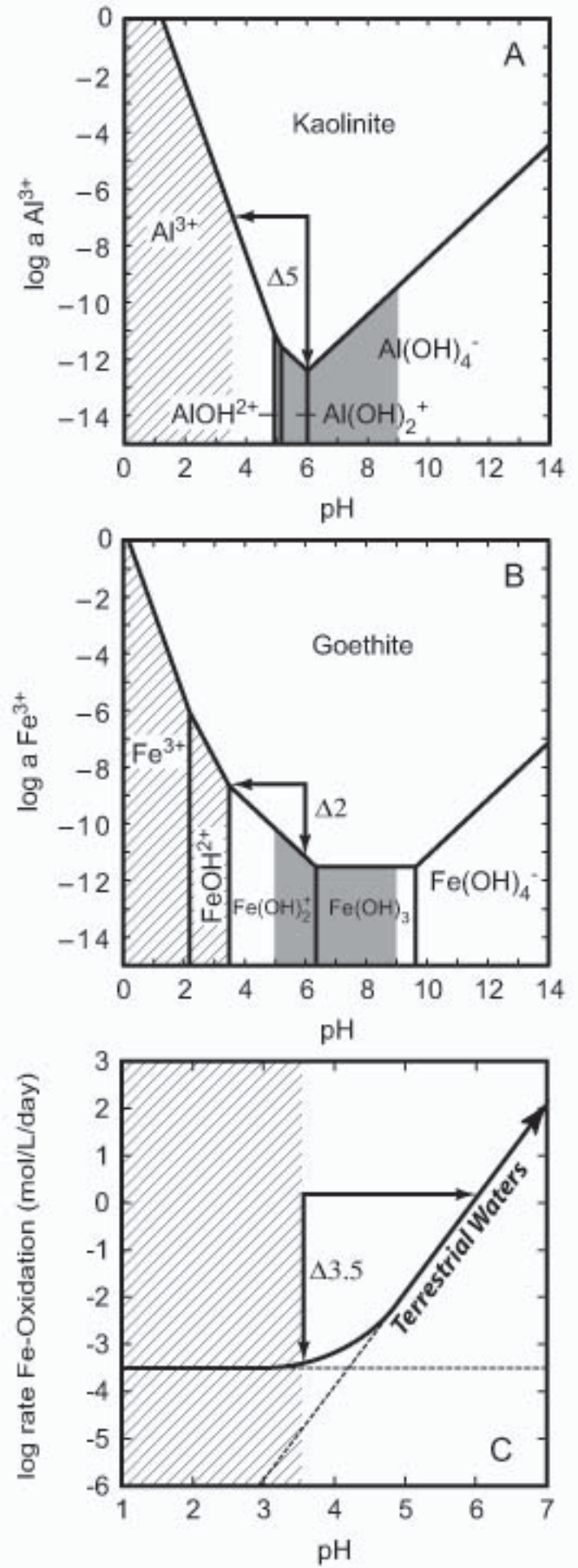
A
Kaolinite
log a Al3+
Al3+
Δ5
Al(OH)4-
AlOH2+
Al(OH)2+
pH
B
Goethite
log a Fe3+
Fe3+
FeOH2+
Δ2
Fe(OH)2+
Fe(OH)3
Fe(OH)4-
pH
C
log rate Fe-Oxidation (mol/L/day)
Δ3.5
Terrestrial Waters
pH

TABLE 1

Oxides (weight %)	LA Basalt[1/]	LA Calculated Residue[2/]	PFS Basalt[1/]	PFS Calculated Residue[2/]	Element (mol/L)	LA Solution B2-10[3/]	PFS Solution A (331 hrs)[3/]
SiO_2	49.0	58.0	48.7	54.9	Si	4.22×10^{-3}	7.91×10^{-2}
TiO_2	1.27	0.17	1.16	1.33	Ti	1.63×10^{-4}	1.20×10^{-3}
Al_2O_3	10.9	0.43	10.3	12.8	Al	2.30×10^{-3}	5.54×10^{-4}
FeO_T	20.4	24.5	19.2	13.2	Fe	1.44×10^{-3}	1.21×10^{-1}
MnO	0.43	0.68	0.49	0.34	Mn	1.93×10^{-5}	3.06×10^{-3}
MgO	3.34	5.82	7.66	3.59	Mg	2.04×10^{-4}	1.19×10^{-1}
CaO	9.7	9.67	7.07	8.61	Ca	1.05×10^{-3}	3.23×10^{-3}
Na_2O	2.32	0.69	3.56	4.43	Na	7.07×10^{-4}	4.58×10^{-4}
K_2O	0.26	NA	0.67	0.83	K	NA	9.31×10^{-5}
Mass (g)	0.1074	0.05	0.1502	0.12	Mass (g)	100	1.5

1/ Bulk compositions and mass of synthetic Los Angeles (LA) basalt and Pathfinder Soil (PFS) basalt from Hurowitz et al. [in press] and Tosca et al. [2004], respectively.
2/ Calculated compositions and mass of residue remaining from experimental alteration of LA and PFS basalts.
3/ Solution compositions and mass of effluent samples B2-10 and PFS Solution-A (331 hours) from Hurowitz et al. [in press] and Tosca et al. [2004], respectively.

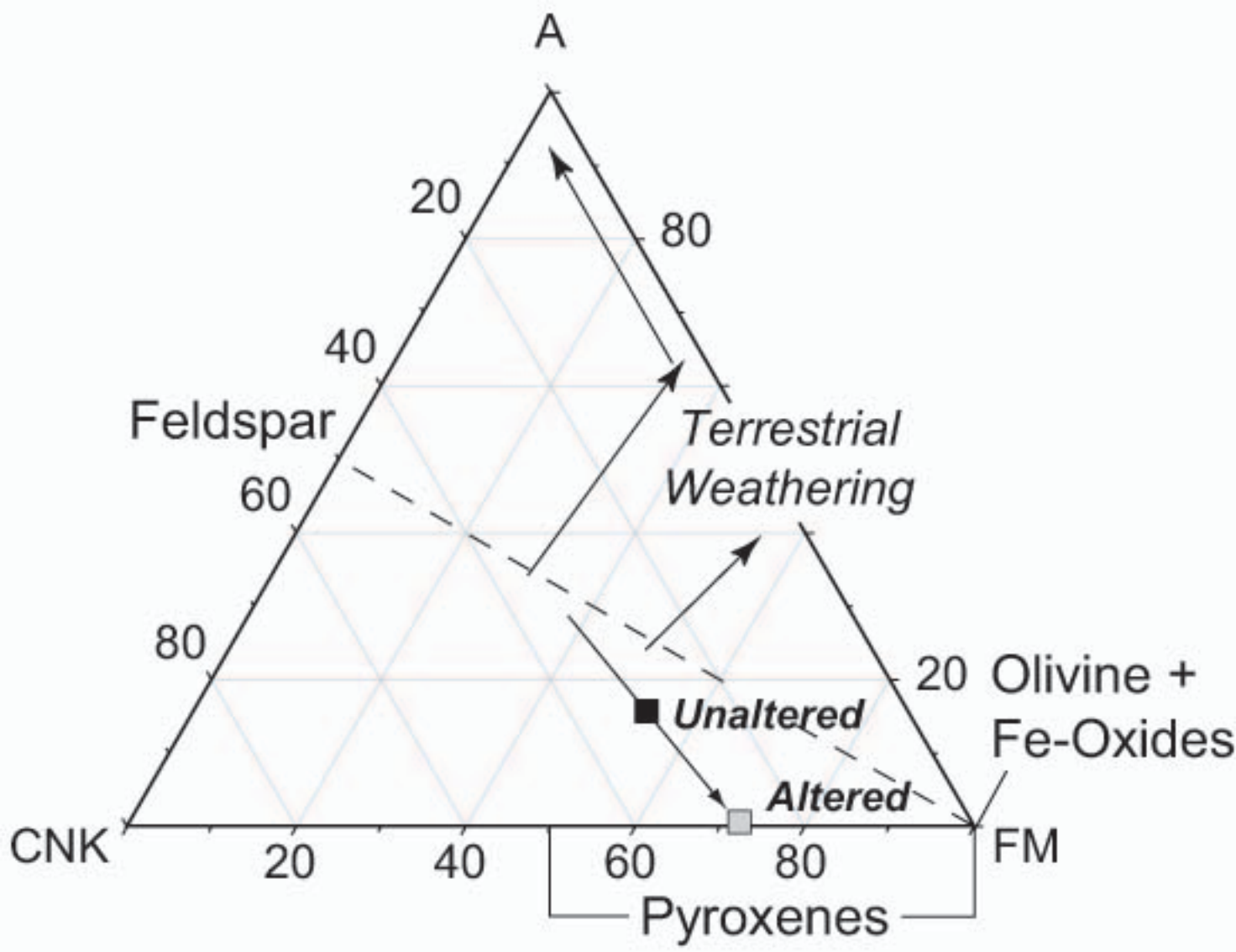
A
20
40
60
80
Feldspar
Terrestrial
Weathering
20
Olivine +
Fe-Oxides
Unaltered
Altered
CNK
20
40
60
80
FM
Pyroxenes

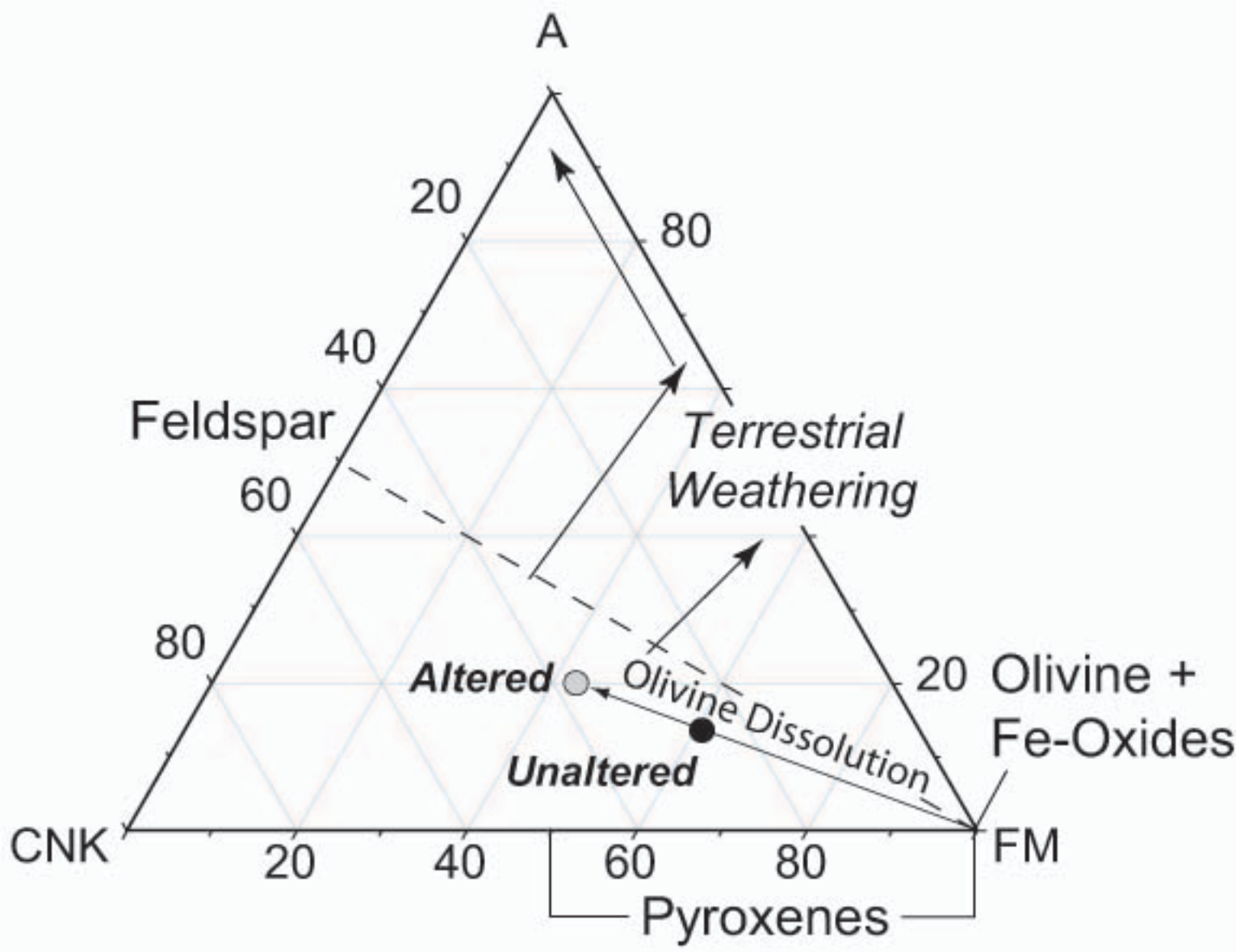
A
20
40
60
80
Feldspar
Terrestrial
Weathering
Altered
Olivine Dissolution
Unaltered
20
Olivine +
Fe-Oxides
CNK
20
40
60
80
FM
Pyroxenes

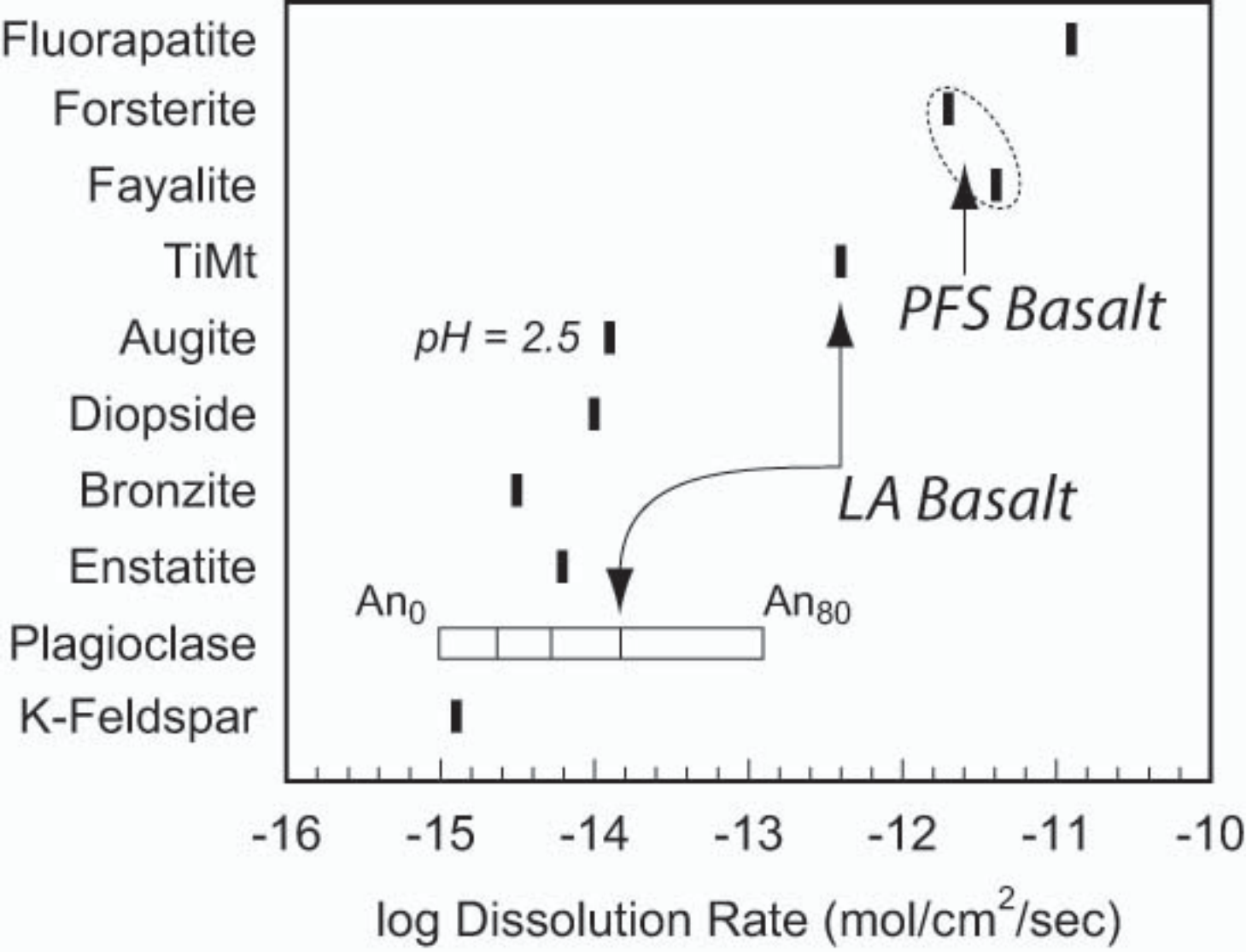
Fluorapatite
Forsterite
Fayalite
TiMt
Augite
Diopside
Bronzite
Enstatite
Plagioclase
K-Feldspar
pH = 2.5
PFS Basalt
LA Basalt
An0
An80
-16
-15
-14
-13
-12
-11
-10
log Dissolution Rate (mol/cm2/sec)

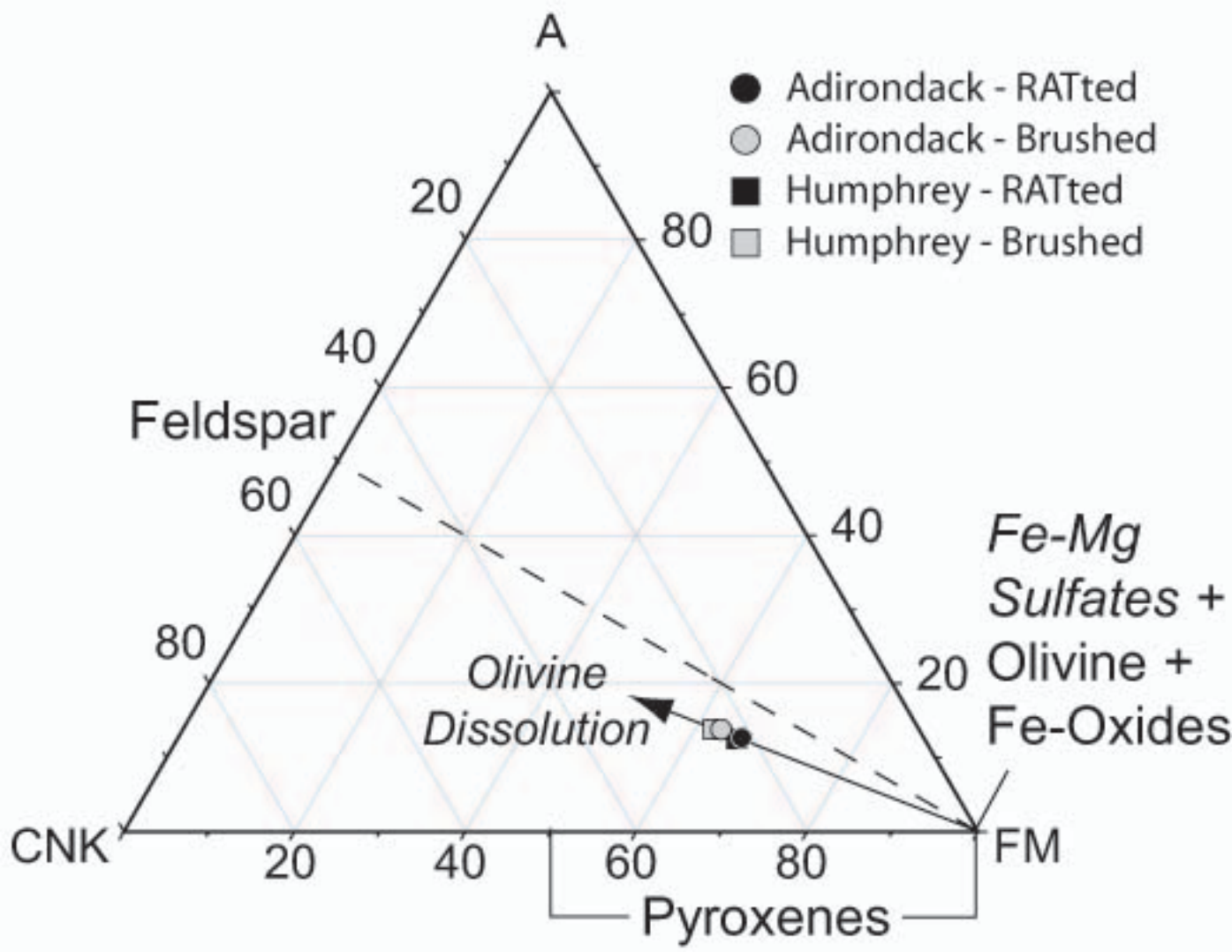
A
Adirondack - RATted
Adirondack - Brushed
Humphrey - RATted
Humphrey - Brushed
20
40
60
80
Feldspar
Olivine
Dissolution
Fe-Mg
Sulfates +
Olivine +
Fe-Oxides
CNK
FM
Pyroxenes

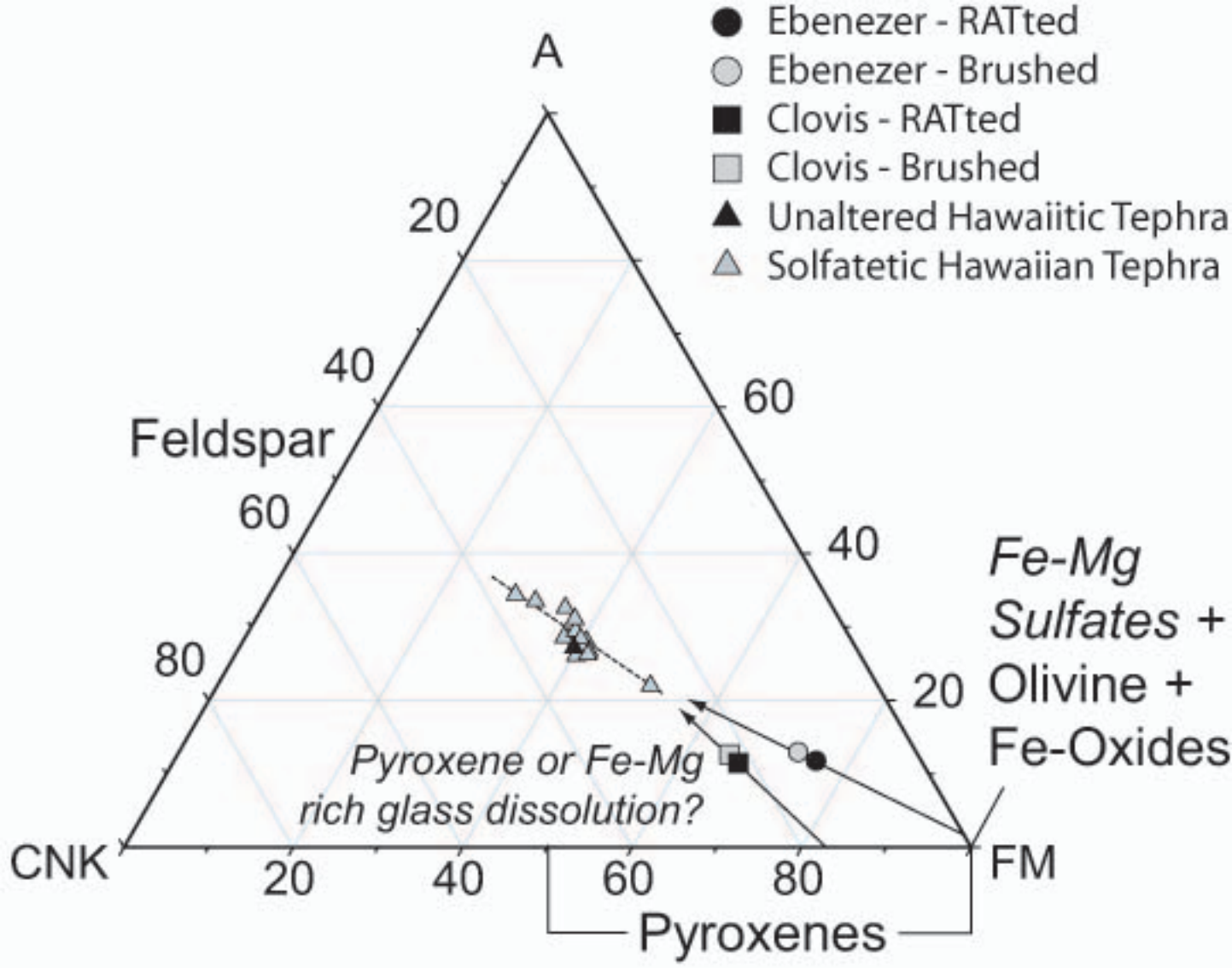
Ebenezer - RATted
Ebenezer - Brushed
Clovis - RATted
Clovis - Brushed
Unaltered Hawaiitic Tephra
Solfatetic Hawaiian Tephra
A
20
40
60
80
Feldspar
Fe-Mg
Sulfates +
Olivine +
Fe-Oxides
Pyroxene or Fe-Mg
rich glass dissolution?
CNK
FM
Pyroxenes

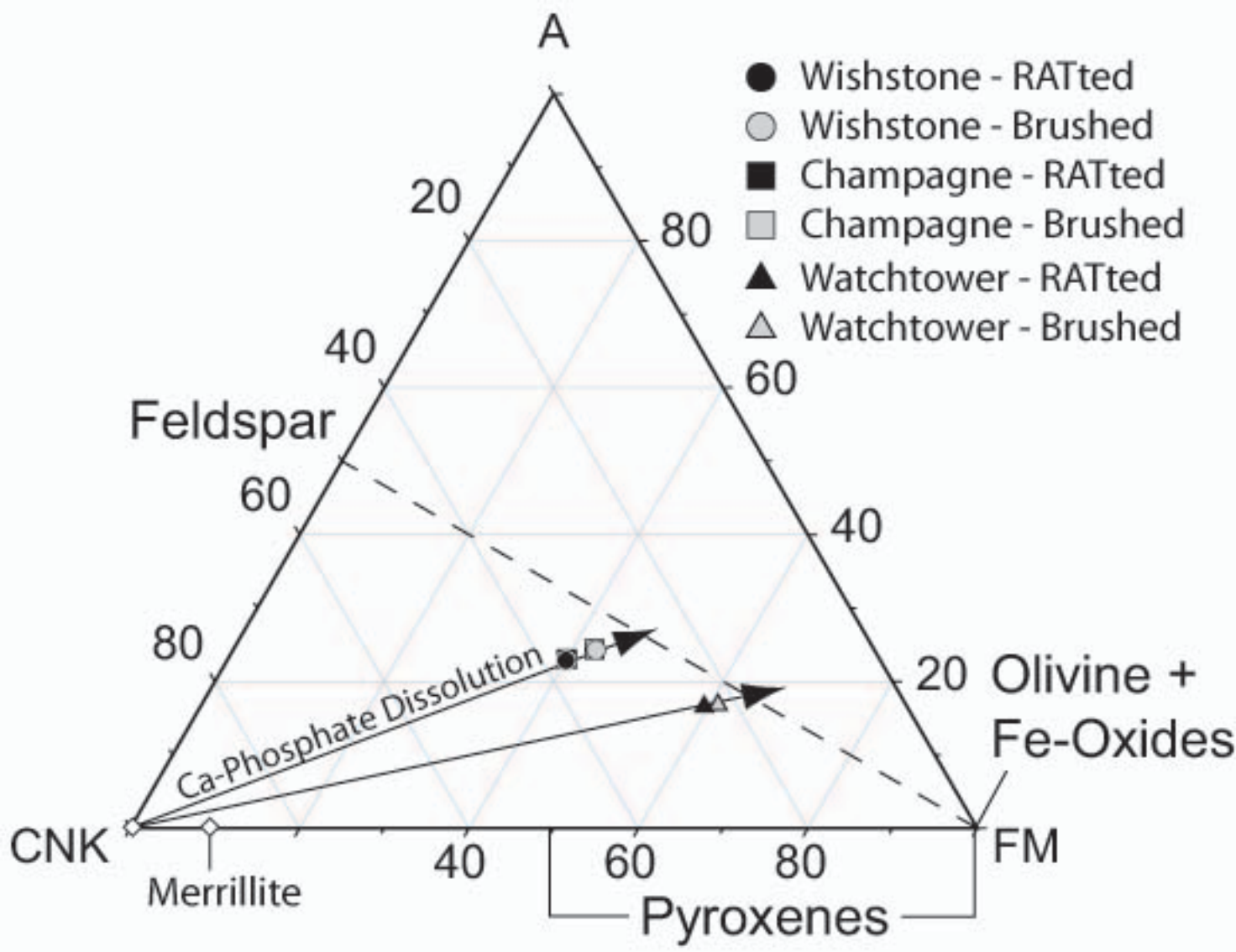
A
Wishstone - RATted
Wishstone - Brushed
Champagne - RATted
Champagne - Brushed
Watchtower - RATted
Watchtower - Brushed
20
40
60
80
Feldspar
Ca-Phosphate Dissolution
Olivine +
Fe-Oxides
CNK
Merrillite
FM
Pyroxenes

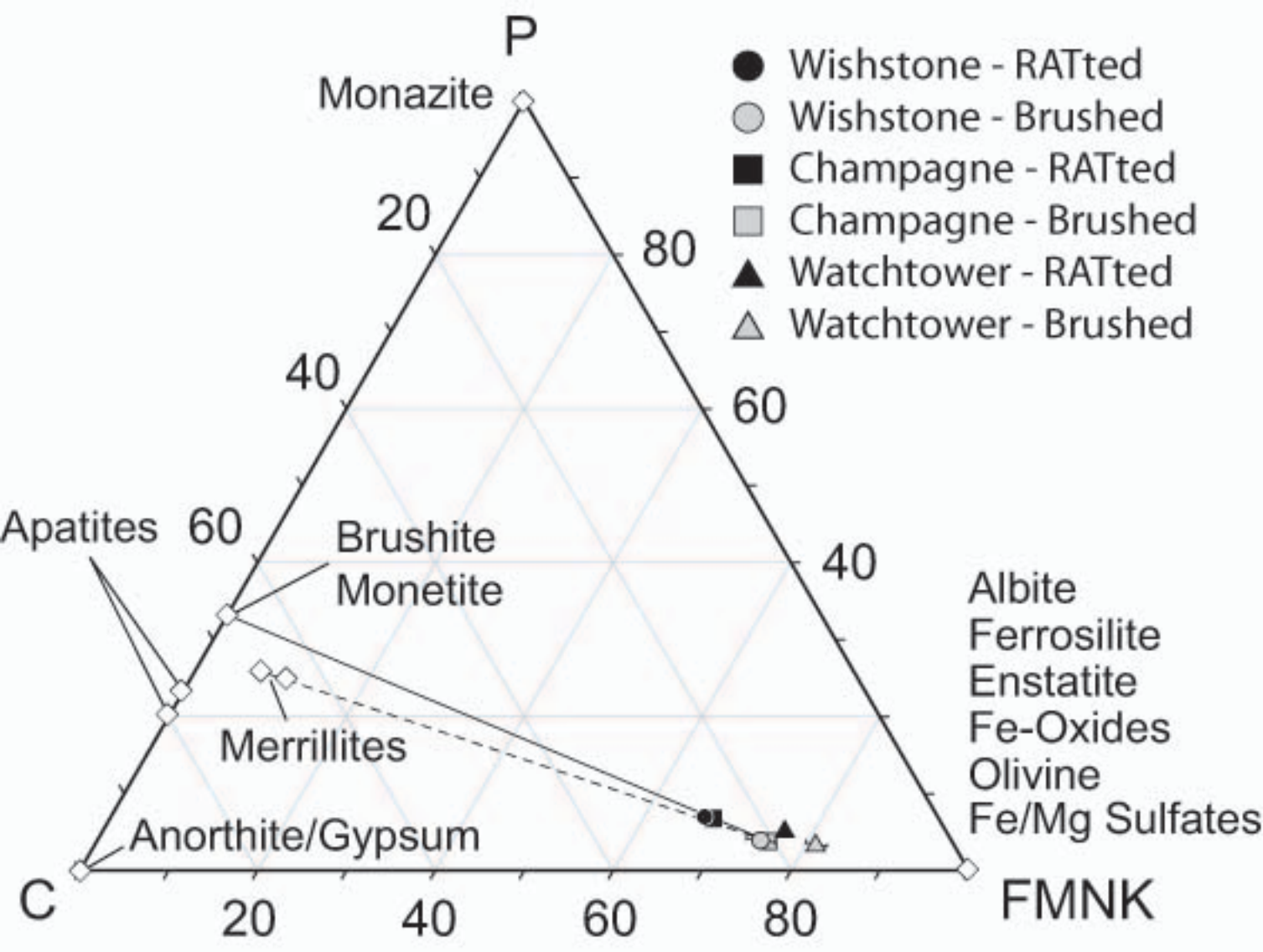
P
Monazite
20
40
60
80
Wishstone - RATted
Wishstone - Brushed
Champagne - RATted
Champagne - Brushed
Watchtower - RATted
Watchtower - Brushed
Apatites
60
Brushite
Monetite
40
Albite
Ferrosilite
Enstatite
Fe-Oxides
Olivine
Fe/Mg Sulfates
Merrillites
Anorthite/Gypsum
C
20
40
60
80
FMNK

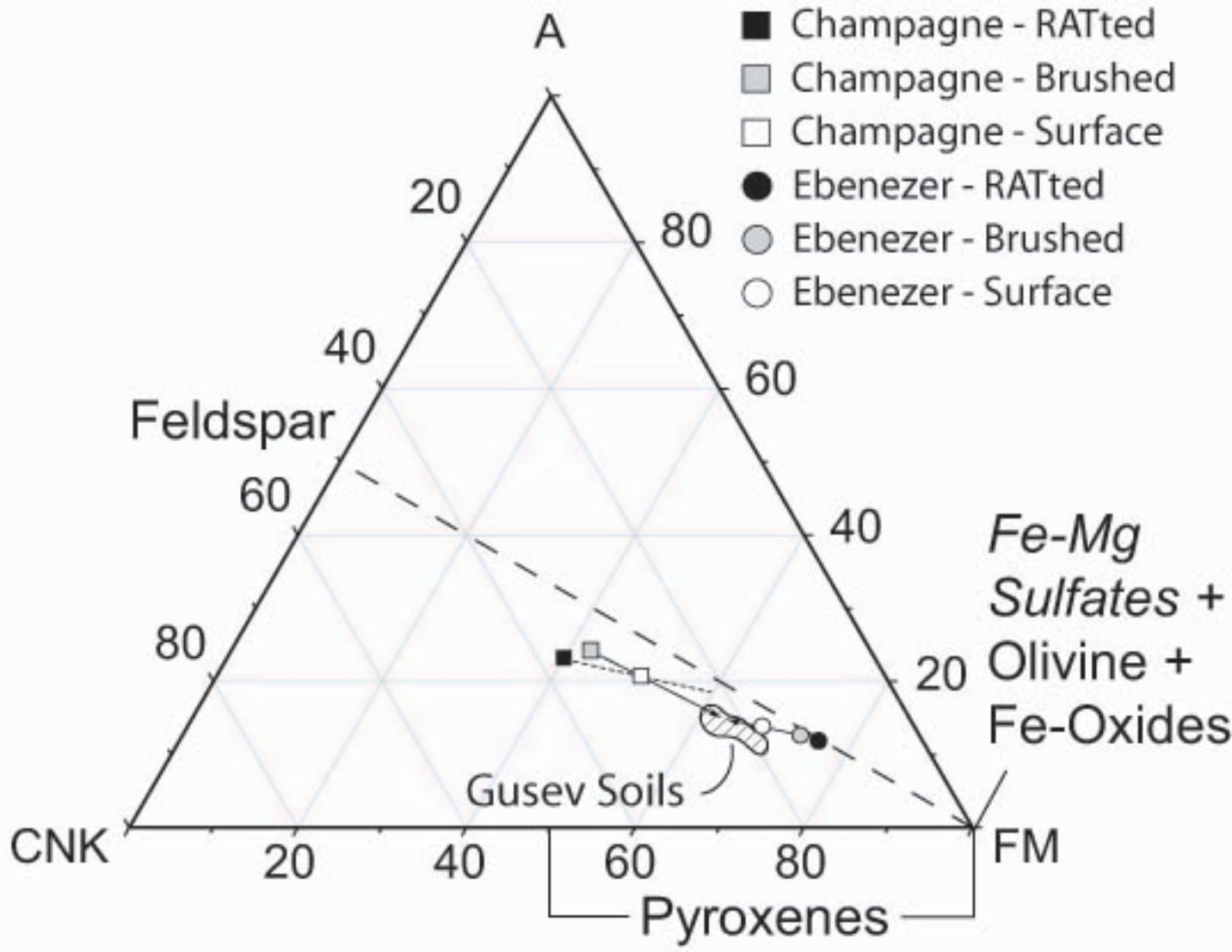
A
Champagne - RATted
Champagne - Brushed
Champagne - Surface
Ebenezer - RATted
Ebenezer - Brushed
Ebenezer - Surface
20
40
60
80
Feldspar
Fe-Mg Sulfates + Olivine + Fe-Oxides
Gusev Soils
CNK
FM
Pyroxenes

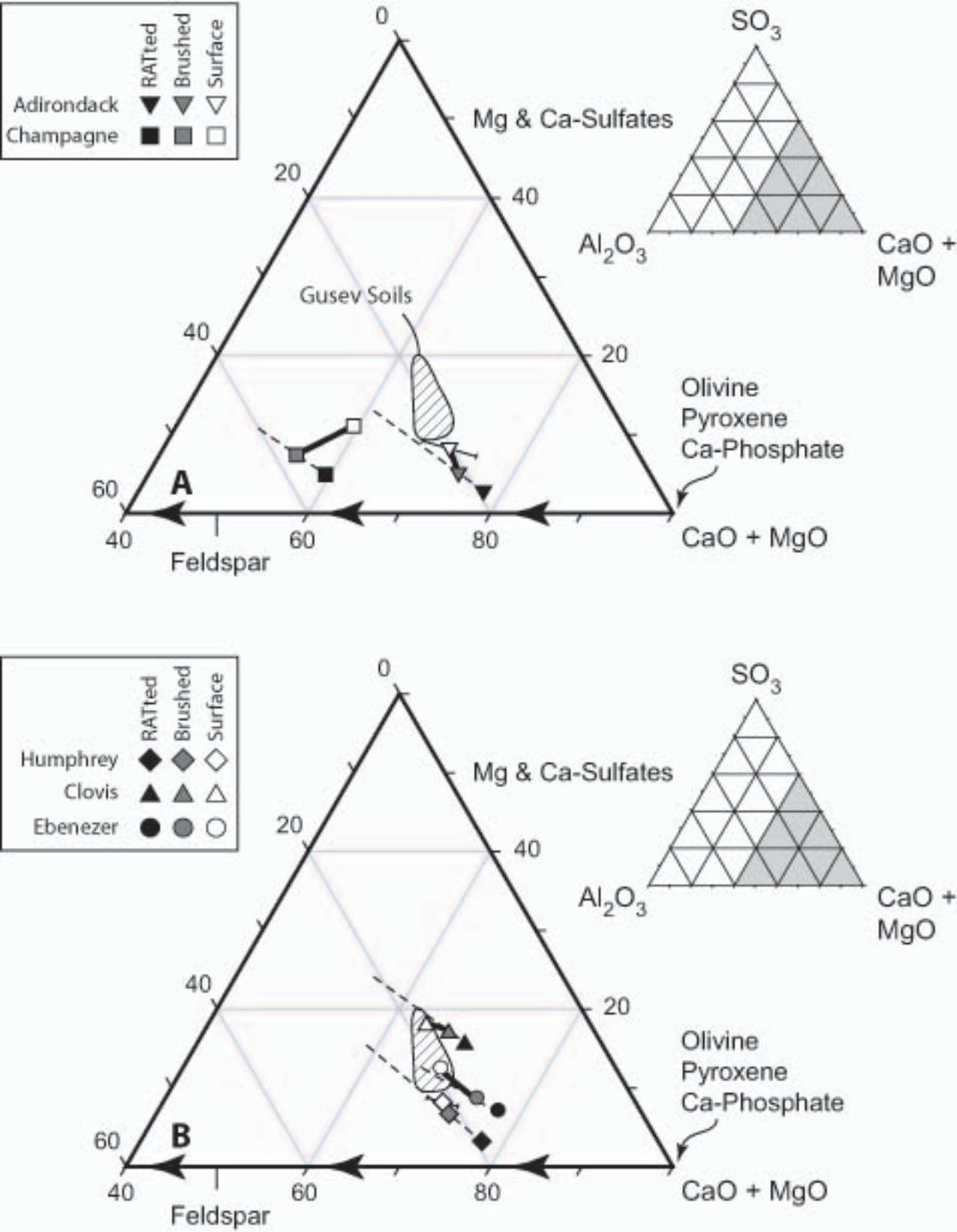
RATted
Brushed
Surface
Adirondack
Champagne
Humphrey
Clovis
Ebenezer
Mg & Ca-Sulfates
Gusev Soils
Olivine
Pyroxene
Ca-Phosphate
CaO + MgO
Feldspar
SO3
Al2O3
CaO + MgO
A
B
0
20
40
60
80

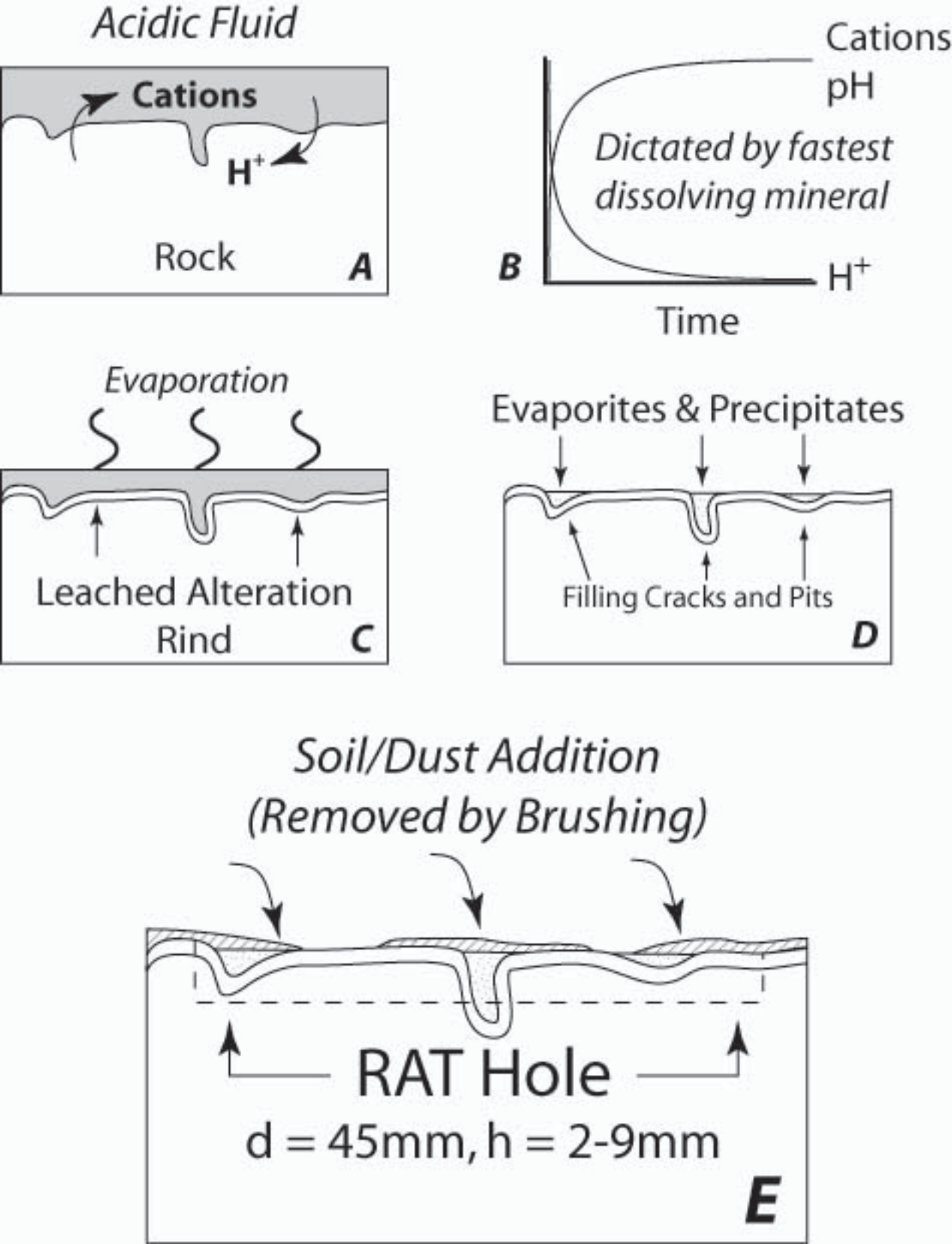
Acidic Fluid
Cations
H+
Rock
A
Cations
pH
Dictated by fastest dissolving mineral
B
H+
Time
Evaporation
Leached Alteration Rind
C
Evaporites & Precipitates
Filling Cracks and Pits
D
Soil/Dust Addition
(Removed by Brushing)
RAT Hole
d = 45mm, h = 2-9mm
E

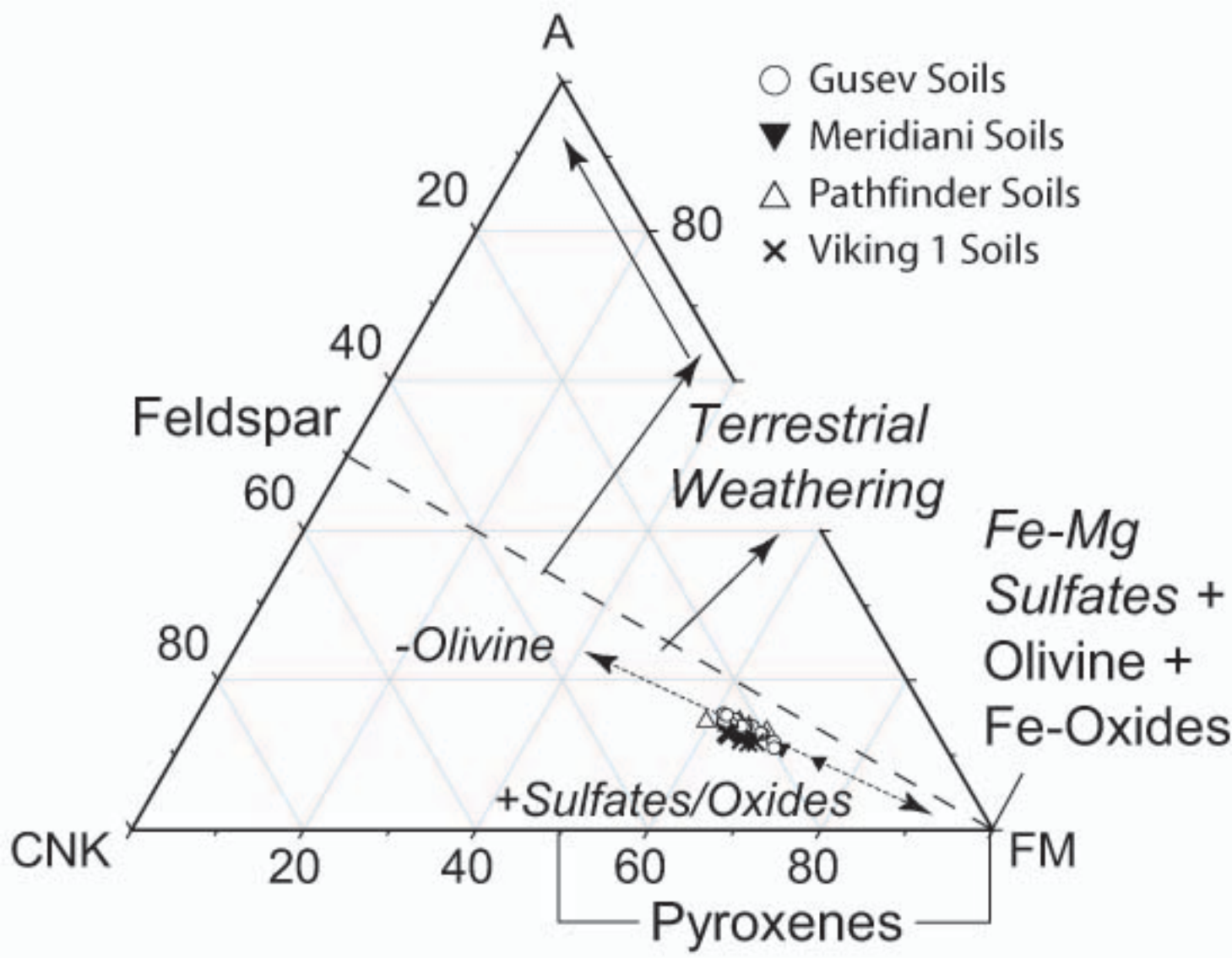
A
Gusev Soils
Meridiani Soils
Pathfinder Soils
Viking 1 Soils
20
40
60
80
Feldspar
Terrestrial
Weathering
Fe-Mg
Sulfates +
Olivine +
Fe-Oxides
-Olivine
+Sulfates/Oxides
CNK
FM
20
40
60
80
Pyroxenes